

1           **Beneficial Effects of Moderate Hepatic Activin A Expression on**  
2           **Metabolic pathways, Inflammation, and Atherosclerosis**

3  
4   Huan Liu, PhD, Margaret Hallauer Hastings, PhD, Robert Kitchen, PhD, Chunyang Xiao, Ph.D.,  
5   Justin Ralph Baldovino Guerra, B.S., Alexandra Kuznetsov, B.A., Anthony Rosenzweig, M.D.\*

6  
7   *Short title: Beneficial Effects of Activin A in Atherosclerosis*

8   *Total Word Count:7343*

9   Cardiovascular Research Center, Massachusetts General Hospital, and Harvard Medical School,  
10   Boston, MA, 02114, USA.

11  
12   \*Correspondence to:

13           Anthony Rosenzweig, MD  
14           Corrigan Minehan Heart Center  
15           Division of Cardiology,  
16           Massachusetts General Hospital, GRB810,  
17           55 Fruit St, Boston, MA 02114  
18           Email: arosenzweig@partners.org  
19

20 **BACKGROUND:** Atherosclerosis is an inflammatory vascular disease marked by hyperlipidemia  
21 and hematopoietic stem cell (HSC) expansion. Activin A, a member of the  
22 Activin/GDF/TGF $\beta$ /BMP family is broadly expressed and increases in human atherosclerosis, but  
23 its functional effects *in vivo* in this context remain unclear.

24 **METHODS:** We studied LDLR<sup>-/-</sup> mice on a Western diet for 12 weeks and used adeno-associated  
25 viral vectors with a liver-specific thyroxine binding globulin (TBG) promoter to express Activin  
26 A or GFP (control). Atherosclerotic lesions were analyzed by oil red staining. Blood lipid profiling  
27 was performed by HPLC (High Performance Liquid Chromatography), and immune cells were  
28 evaluated by flow cytometry. Liver RNA-sequencing was performed to explore the underlying  
29 mechanisms.

30 **RESULTS:** Activin A expression decreased in both livers and aortae from LDLR<sup>-/-</sup> mice fed a  
31 Western diet compared with chow. AAV-TBG-Activin A increased Activin A hepatic expression  
32 (~10-fold at 12-weeks,  $p < 0.0001$ ) and circulating Activin A levels (~2000pg/ml vs ~50pg/ml,  
33  $p < 0.001$ , compared with controls). Hepatic Activin A expression decreased plasma total and low-  
34 density lipoprotein (LDL) cholesterol (~60% and ~40%, respectively), reduced inflammatory cells  
35 in aortae and proliferating hematopoietic stem cells (HSC) in bone marrow, and reduced  
36 atherosclerotic lesion area in the aortic arch by ~60%. Activin A also attenuated liver steatosis and  
37 expression of the lipogenesis genes, Srebp1 and Srebp2. RNA sequencing revealed Activin A not  
38 only blocked expression of genes involved in hepatic *de novo* lipogenesis but also fatty acid uptake,  
39 and liver inflammation. In addition, Activin A expressed in the liver also reduced white fat tissue  
40 accumulation, decreased adipocyte size, and improved glucose tolerance.

41 **CONCLUSIONS:** Our studies reveal hepatic Activin A expression reduces inflammation, HSC  
42 expansion, liver steatosis, circulating cholesterol, and fat accumulation, which likely all contribute  
43 to the observed protection against atherosclerosis. The reduced Activin A observed in LDLR<sup>-/-</sup>  
44 mice on a Western diet appears maladaptive and deleterious for atherogenesis.

45 **Key words:** Activin A, atherosclerosis, HSC, inflammation, cholesterol

46

47 **Non-standard Abbreviations and Acronym**

48 TBG-thyroxine binding globulin

49 CVD-cardiovascular diseases

50 LDL-low density lipoprotein

51 VLDL-very low-density lipoprotein

52 oxLDL- (oxidized- LDL)

53 AAV-adeno-associated virus

54 FST-Follistatin

55 HSC- hematopoietic stem cell

56 LtHSC-long-term hematopoietic stem cell

57 StHSC-short-term hematopoietic stem cell

58 MPP-multipotential progenitor cells

59 PMN- polymorphonuclear cells

60 DEG- differentially expressed genes

61 FAs-fatty acids

62

63

64

65

66

67

68

69

70

## 71 **Introduction**

72 Cardiovascular diseases (CVD) are the leading cause of death worldwide<sup>1</sup>. Atherosclerosis is a  
73 progressive CVD characterized by accumulation of lipid plaques in arterial walls with  
74 inflammation and hematopoietic stem cell (HSC) expansion<sup>2,3</sup>, and often driven by increased low  
75 density lipoprotein (LDL) cholesterol<sup>4</sup>. Understanding better the mechanisms of atherosclerosis  
76 and identifying potential new therapeutic approaches to this condition has important clinical  
77 implications.

78 The liver is central to lipid metabolism including involves in uptake, esterification, oxidation,  
79 and secretion of fatty acids (FAs) with important downstream effects on systemic inflammation  
80 and metabolism. The liver is also responsible for synthesis, uptake, storage, and efflux of  
81 cholesterol, essential for multiple biological processes<sup>5-7</sup>. Cholesterol, triglycerides, and other  
82 lipids are assembled in the liver into lipoproteins, which are transported to peripheral tissues  
83 through the circulation<sup>5,6</sup>. Hepatic free cholesterol can be esterified, incorporated into very low-  
84 density lipoprotein (VLDL) particles, secreted into the bloodstream, further converted into smaller  
85 LDL particles, and then oxidized and taken up by macrophages to form foam cells, which promote  
86 the formation of atherosclerotic plaques<sup>5,6</sup>. Thus, hepatic lipid metabolism and cholesterol  
87 synthesis are essential for health of the organism but also have potential deleterious effects, such  
88 as atherosclerosis.

89 Hepatic sterol regulatory element binding proteins (SREBPs) play important roles in  
90 atherosclerosis. These include the transcription factors, Srebp1a, Srebp1c (alternative splicing  
91 products of Srebp1, also known as Srebf1), which are involved in synthesis of cholesterol, fatty  
92 acids, and triglycerides (TGs), and Srebp2 (Srebf2), which regulates expression of HMG-CoA (3-  
93 hydroxy-3-methylglutaryl-CoA) reductase, the target of statins, and the LDL receptor (LDLR)<sup>8</sup>.

94 Hepatic Srebp1c expression increases atherogenic lipoprotein profiles and accelerates  
95 atherosclerosis in LDLR<sup>-/-</sup> mice<sup>9</sup>. Concordantly, an inhibitor of Srebp processing reduces  
96 atherosclerosis<sup>10</sup>. Similarly, GPR146 deficiency reduces hepatic Srebp2 activity and protects  
97 against atherosclerosis<sup>11</sup>.

98 Activin A is a member of Activin/GDF/TGF $\beta$ /BMP protein family. Many members of this  
99 family, including Activin A, drive a metabolic switch from an anabolic to catabolic state. Activin  
100 A signals through type I (ACTR1B [ALK4], ACTR1C [ALK7] or TGFBR1) and type II  
101 (ACVR2A, ACVR2B, and BMPR2) receptors to induce Smad2/3 phosphorylation and nuclear  
102 translocation regulating gene expression<sup>12, 13</sup>. Follistatin (FST) is induced by Activin signaling  
103 and antagonizes its ACVR receptor binding site<sup>14</sup>, forming a negative feed-back loop<sup>15</sup>. Activin  
104 A can also form a non-signaling complex with type I (ACVR1A, ALK2) and type II receptors<sup>16-</sup>  
105 <sup>18</sup>.

106 The role of Activin A in atherosclerosis is unclear. On one hand, Activin A is expressed in the  
107 intima in early atherosclerotic lesions and elevated further in lesions of advanced atherosclerotic  
108 patients<sup>19, 20</sup>. Plasma Activin A is increased in angina patients (~500 pg/ml) compared with  
109 controls (~300 pg/ml)<sup>19-21</sup>. These observations suggest Activin A could contribute to  
110 atherosclerosis progression. On the other hand, *in vitro* studies demonstrate that Activin A inhibits  
111 foam cell formation in Thp1 and Raw 264.7 macrophages<sup>22, 23</sup>, thought to model an early step in  
112 atherogenesis, while FST promotes foam cell formation in Thp1 macrophages<sup>24, 25</sup>. Exogenous  
113 Activin A has also been reported to reduce neointimal hyperplasia in a femoral artery cuff murine  
114 model *in vivo*<sup>26</sup>. These studies suggest Activin A may be anti-atherogenic and focus on its role in  
115 vessel wall constituents. Thus, we lack an understanding of the *in vivo* effects of Activin in  
116 atherosclerosis and the role of different sites of expression.

117 Here we find that Activin A is highly expressed in aorta and liver but decreases in both in  
118 LDLR<sup>-/-</sup> mice fed a Western diet compared with those fed chow. Hepatic Activin A expression  
119 mediated by an adeno-associated viral vector in LDLR<sup>-/-</sup> atherosclerotic mice increased circulating  
120 Activin A levels (~2000 pg/ml vs ~50pg/ml, p<0.0001) and protected against atherosclerosis by  
121 reducing cholesterol, decreasing inflammation, and reducing proliferating HSCs. Mechanistically,  
122 hepatic Activin A reduced liver Srebp1/Srebp2 expression, pathways involved in hepatic  
123 lipogenesis and fatty acid uptake, as well as liver steatosis. In addition, hepatic Activin A reduced  
124 body fat accumulation and improved glucose tolerance. We conclude that the reduction in hepatic  
125 Activin A observed on a Western diet is maladaptive and could represent an evolutionary vestige  
126 perhaps valuable in calorie-poor environment but potentially maladaptive amidst caloric  
127 abundance. Whether AAV8-TBG-Activin A has therapeutic potential in atherosclerosis and  
128 related metabolic diseases may warrant further investigation.

129

## 130 **Methods**

131 The data, methods, and study materials used to conduct the research will be available from the  
132 corresponding author upon reasonable request.

## 133 **Animal Studies**

134 All mouse experiments were performed in accordance with the NIH Guide for the Care and Use  
135 of Laboratory Animals and approved by the Institutional Animal Care and Use Committee  
136 (IACUC) of Massachusetts General Hospital.

137 For the atherosclerosis model, 8-week-old male LDLR<sup>-/-</sup> (#002207, body weight ~24-25g)  
138 obtained from Jackson Laboratory were injected via tail vein with AAV8-TBG-GFP or AAV8-

139 TBG-Activin A viruses at  $2 \times 10^{10}$  genome copies/mouse. After 1 week, mice were fed a high  
140 cholesterol Western diet (Envigo Teklad, TD.96121) or standard chow diet for 12 weeks. Mice  
141 were fasted overnight before euthanasia.

142 A detailed description of the methods and supporting data are available in the Online  
143 Supplemental materials.

#### 144 **Statistical Analysis**

145 Data are expressed as mean $\pm$ SEM and analyzed using GraphPad Prism 8 (GraphPad Software)  
146 by unpaired Student t-tests.  $p < 0.05$  was considered significant. \* $p < 0.05$ , \*\* $p < 0.005$ , and  
147 \*\*\* $p < 0.001$ .

148

#### 149 **Results**

##### 150 **Activin A mRNA decreases in aorta and liver in LDLR<sup>-/-</sup> mice fed a Western diet**

151 We examined plasma Activin A levels as well as the expression of the Activin A transcript in  
152 liver and aorta, and how these were affected by hyperlipidemia. Plasma Activin A levels were  
153 increased in LDLR<sup>-/-</sup> mice fed a Western diet compared with chow (Figure 1A) while plasma  
154 Follistatin (FST) levels were similarly undetectable in all mice (data not shown). Baseline Activin  
155 A mRNA levels measured by QPCR were high in aorta and liver relative to other organs tested  
156 (Figure S1A). Surprisingly, given previous reports of increased Activin A expression in  
157 atherosclerosis<sup>19-21</sup>, Activin A mRNA levels decreased in both aortae and livers from LDLR<sup>-/-</sup> mice  
158 fed a Western diet compared with chow (Figure 1B-1C). In contrast, FST was expressed most  
159 highly in muscle and aorta, and at lower levels in liver (Figure S1B) and was unaffected by diet  
160 (Figure 1B-1C). Consistent with these observations, we found that oxidized LDL (oxLDL)

161 decreased Activin A but not FST mRNA in primary peritoneal macrophages and the Hepa 1-6  
162 hepatic carcinoma cell line (Figure 1D-1E). Together these observations suggest the Activin  
163 pathway is suppressed in the liver and aorta, and this may be a direct effect of oxLDL.

#### 164 **Activin A protects against atherosclerosis *in vivo***

165 We generated AAV8 vectors using the TBG promoter to drive liver-specific<sup>27, 32-34</sup> expression  
166 of Activin or GFP. We confirmed TBG-driven Activin A mRNA expression in HepG2 cells and  
167 protein in the media, as well as induction of Smad2/3 phosphorylation that was blocked by FST-  
168 315, the circulating isoform of FST (Figure S2A). Similar to recombinant Activin A protein<sup>24, 25</sup>,  
169 Activin A from HepG2 conditioned media also reduced oxLDL uptake by peritoneal macrophages  
170 *in vitro* (Figure 2A-2B). Thus, the AAV8-TBG-Activin A vector effectively induces Activin A  
171 expression and functional protein secretion.

172 *In vivo* studies confirmed that TBG-driven GFP expression was specific to the liver (Figure  
173 S2B) and TBG also mediated hepatic Activin A expression that induced Smad2/3 phosphorylation,  
174 and increased circulating plasma Activin A (Figure S2C-S2E). LDLR<sup>-/-</sup> mice were injected with  
175 AAV8-TBG-GFP (control) or AAV8-TBG-Activin A, and then fed a western diet for 12 weeks to  
176 induce early-stage atherosclerosis (Figure 2C). Hepatic Activin A expression induced Smad2/3  
177 phosphorylation and expression of the downstream target gene FST in the liver but not aorta  
178 (Figure 2D-2F and S2F). Notably, Activin receptors, ACVR1b and ACVR2b, dramatically  
179 decreased and ACVR2a showed a nonsignificant trend toward decreasing in Activin-expressing  
180 mice compared with controls (Figure S2G). Plasma Activin A increased in AAV8-TBG-Activin  
181 A treated mice compared to controls (Figure 2G). Of note, plasma Activin A levels in control mice  
182 fed the Western diet were higher than chow diet (Figure 1A). However, plasma Activin A levels  
183 seen in Activin A-expressing mice fed a Western diet were even higher (Figure 2G). The molecular



184 weight of the FST band detected in the liver (<35kd) was smaller than FST315 (>35kd), suggesting  
185 it may correspond to the FST288 isoform, which is limited to tissue and not secreted into the  
186 circulation. Indeed, plasma FST levels remained at background levels (data not shown), suggesting  
187 the ratio of plasma Activin A/FST was increased in the Activin A expressing mice compared with  
188 controls. Surprisingly, Activin A did not induce liver injury and plasma ALT (or SGPT for  
189 Serum Glutamic-Pyruvic Transaminase) decreased in Activin-expressing mice compared with  
190 controls (Figure 2H).

191 Oil red staining demonstrated that Activin A expression dramatically decreased atherosclerotic  
192 plaques in the aortic arch by ~60% (Figure 2I-2J). In addition, flow cytometry revealed that Ly-  
193 6C<sup>high</sup> monocytes, F4/80+ macrophages and Ly-6G+ neutrophils were all substantially decreased  
194 in aortae from Activin A-expressing mice compared with controls (Figure 2K-2L), suggesting both  
195 lesion size and inflammation were reduced by Activin A. Hepatic Activin A expression  
196 dramatically decreased plasma total cholesterol (>50%), LDL (~40%), and triglycerides (>80%)  
197 (Figure 2M-2O), without altering HDL (Figure 2P); thus, reducing the LDL/HDL ratio (Figure  
198 2Q). Taken together, hepatic Activin A protected against atherosclerosis *in vivo* and this was  
199 associated with a substantial decline in circulating atherogenic lipid levels (LDL-C and TGs)  
200 without a change in HDL or increased liver injury.

201 We next used flow cytometry to investigate the effect of Activin A on HSCs. Activin A  
202 decreased the absolute number of bone marrow LSK (Lin-CD45+Sca1+c-Kit+) cells, the  
203 population that includes HSCs<sup>35</sup>, by ~60% (Figure S2H-S2I). In the LSK population, long-term  
204 HSCs (LtHSC, CD135-/CD150+/CD48- LSK(Lin-Sca1+c-Kit+)) differentiate into short-term  
205 HSCs (StHSC, CD135-/CD150-/CD48-LSK) and then multipotent progenitor cells (MPPs)  
206 including MPP2 (CD135-/CD150+/CD48+LSK), MPP3 (CD135-/CD150-/CD48+ LSK) and

207 MPP4 (CD135+/CD150-/CD48+/- LSK)<sup>36</sup>. There was an >80% decrease in L<sup>t</sup>HSC and S<sup>t</sup>HSC  
208 and ~60% decrease in MPP2, MPP3 and MPP4 cells in atherosclerotic mice expressing Activin A  
209 compared with controls (Figure S2H-S2I).

210 To determine whether the decrease in LSK cells is due to an effect on HSC proliferation, we  
211 assessed BrdU incorporation by flow cytometry. LSK cells were dramatically decreased overall  
212 and BrdU<sup>+</sup> LSK cells were reduced ~60% in Activin A-expressing atherosclerotic mice versus  
213 controls (Figure 2R-2S). Thus, Activin A decreased the actively proliferating and the total number  
214 of HSC in atherosclerotic mice.

### 215 **Activin A decreases liver steatosis and inflammation in atherosclerotic mice**

216 We next investigated the effects of AAV8-TBG-Activin A on the liver itself. The accumulation  
217 of excessive lipid droplets is a pathological change known as hepatic steatosis<sup>7</sup>. H&E and oil red  
218 staining revealed accumulation of much smaller lipid droplets in Activin A-expressing livers  
219 compared with controls (Figure 3A-3B). The accumulation of free cholesterol contributes to liver  
220 injury, ER stress, mitochondrial dysfunction, fibrosis inflammation, as well as cholesterol  
221 crystallization in lipid droplets and consequent hepatocyte cell death<sup>37-40</sup>. Activin A expression  
222 decreased hepatic total and free cholesterol by 30% without changing triglycerides, a common and  
223 “safe storage” for fatty acids (Figure 3C-3E). In addition, QPCR demonstrated that Activin A  
224 expression reduced expression of Srebp1 and Srebp2 (Figure 3F), suggesting that Activin A could  
225 inhibit hepatic lipogenesis. Picrosirius Red staining (collagen I and III) demonstrated that fibrosis  
226 was primarily located in lipid droplet-rich regions in control livers but around veins in Activin A  
227 expressing livers (Figure 3A). There was no difference in overall fibrotic area in the two groups  
228 (Figure 3H). Although the Activin A pathway was activated, as indicated by increased FST protein  
229 and Smad2/3 phosphorylation (Figure 2E-2F), fibrosis marker genes Col1a1, Col1a2, Col3a1, and

230 MMP12 were significantly decreased (Figure 3G). In addition, there was a trend toward decreased  
231 expression of the hepatic stellate cell marker gene, *Acta2*, in Activin A expressing livers compared  
232 with controls (Figure 3G). Immunohistochemical staining for CD45 showed that inflammatory  
233 cells were dramatically decreased in Activin A-expressing livers compared with control (Figure  
234 3A and 3I). Furthermore, mRNA levels of inflammatory marker genes *TNF $\alpha$*  and *F4/80* were  
235 decreased in Activin A-expressing liver versus controls (Figure 3J). Collectively, these findings  
236 suggest that Activin A decreased liver steatosis and inflammation without inducing fibrosis in  
237 atherosclerotic mice.

### 238 **Activin A reduced expression of pathways involved in fatty acid uptake, *de novo* lipogenesis** 239 **and lipid associated macrophage recruitment**

240 To identify the mechanisms responsible for the effects of hepatic Activin A, we performed  
241 RNA-sequencing in Activin A-expressing compared with control liver samples. Differential  
242 expression analysis confirmed upregulation of Activin A (also known as *Inhba*) and its target gene  
243 *FST* in Activin A-expressing mice compared with controls (Figure 4A). Overrepresentation  
244 analysis of the differentially expressed genes (DEG) identified “Fatty acid metabolic process”  
245 ranks 1 among the GO Biological Process and “lipid and atherosclerosis” ranks 8 among the  
246 KEGG pathways, and (Figure 4B and S3A), likely contributing to the decreased lipid accumulation  
247 seen in Activin A expressing livers.

248 A heatmap generated based on the DEG list from the “fatty acid metabolic process” GO term  
249 and “lipid and atherosclerosis” KEGG pathway revealed decreases in multiple genes related to *de*  
250 *novo* lipogenesis and fatty acid uptake in Activin A-expressing livers (Figure 4C). *Srebp1* is a  
251 pivotal transcription factor for triglyceride metabolism and *de novo* lipogenesis, which directly  
252 activates the key desaturases for the biosynthesis of monounsaturated fatty acids (MUFA) and

253 polyunsaturated fatty acid (PUFAs), including Scd1 (stearoyl-CoA desaturase 1, primarily in liver),  
254 Scd2 (stearoyl-CoA desaturase 2), and fatty acid desaturase (Fads2) expression<sup>41-43</sup>. By QPCR, we  
255 verified that Scd1/2 and Fads2 were significantly decreased in Activin A-expressing livers  
256 compared with controls (Figure 4D). FABPs are essential for intracellular binding and transport of  
257 fatty acids, as well as cholesterol and phospholipid metabolism<sup>44</sup>. Fabp1 is the major hepatic  
258 FABP, and its deficiency attenuates both diet-induced hepatic steatosis and fibrogenesis<sup>45</sup>. mRNA  
259 levels of Fabp1, Fabp2, Fabp5, and the atherogenic scavenger receptor and fatty acid transporter,  
260 CD36<sup>46, 47</sup>, were all decreased in Activin A-expressing liver compared with controls (Figure 4E),  
261 as were the corresponding protein levels (Figure 4G-4H). Consistently, Activin A also inhibits  
262 Srebp1, Srebp2, Fabp5 in Hepa 1-6 cells with oxLDL treatment *in vitro*. (Figure S3B). Oleic acid  
263 (OA, a monounsaturated omega-9 fatty acid) is a potent inducer of triglyceride synthesis and  
264 storage. Activin A reduced OA-induced -fatty acid uptake in Hepa 1-6 cells *in vitro*, while this  
265 effect was rescued with a neutralizing Activin A antibody (Figure S3C-S3D). Multiple  
266 differentially-regulated genes have been reported to play roles in lipid metabolism or to promote  
267 atherosclerosis, such as GDF15<sup>48, 49</sup>, IRF7<sup>50</sup>, Cyba<sup>51</sup>, Cybb<sup>52</sup>, Fas<sup>53, 54</sup>, Vcam1<sup>55</sup> and TLR2<sup>56</sup>  
268 (Figure 4C). Expression of these genes was dramatically reduced in Activin A-expressing liver  
269 (Figure 4F). Thus, Activin A likely blocks both *de novo* lipogenesis and fatty acid uptake to protect  
270 against liver steatosis, free cholesterol accumulation, and associated atherosclerosis (Figure 6F).

271 A recent report showed that adenoviral expression of the glycoprotein NMB (Gpnmb, also  
272 known as DC-HIL) in hepatocytes promotes lipogenesis in white adipose tissue (WAT) and  
273 exacerbates obesity and insulin resistance<sup>57</sup>. Gpnmb is also a core component of Trem2<sup>high</sup>CD9<sup>+</sup>  
274 lipid associated- macrophages (LAM) in the liver and is induced in trans-fat containing AMLN  
275 (amylin liver non-alcoholic steatohepatitis, NASH) diet-induced nonalcoholic steatohepatitis

276 (NASH) liver<sup>58</sup>, while Elafibranor, an agonist of PPAR $\alpha$  and PPAR $\delta$ , reverses NASH and  
277 dramatically decreases Gpnmb protein levels, as well as Trem2, CD9, and Gpnmb mRNA levels  
278 in mice<sup>58</sup>. Interestingly, hepatic Gpnmb mRNA was decreased in Activin A-expressing mice as  
279 (Figure 4A). Interestingly, we found that hepatic Gpnmb mRNA and protein expression were  
280 induced by the Western diet (Figure S3E-S3F) and dramatically decreased in Activin A-expressing  
281 mice (Figure 4A, 4G-4H, 4K). Activin A also attenuated Gpnmb expression and secretion in Hepa  
282 1-6 cells *in vitro* (Figure S3G), suggesting this is a direct effect. Immunofluorescent staining  
283 showed that Gpnmb was colocalized with CD45<sup>+</sup> and F4/80<sup>+</sup> but not hepatocytes, confirming  
284 Gpnmb expression in a macrophage lineage (Figure 4I-4J). Notably, our RNA-seq data also  
285 indicated downregulation of Trem2 (Figure 5A). We next focused on LAM. The LAM marker  
286 genes Trem2 and CD9 are also decreased in Activin A-expressing livers compared with controls  
287 (Figure 4K). Moreover, we confirmed that Activin A expression led to a >3-fold decrease in LAM  
288 Trem2<sup>high</sup> CD9<sup>+</sup> populations in the liver by flow cytometry (Figure 4L-4M). Together, these data  
289 suggest that Activin A expression decreased genes involved in fatty acid uptake, *de novo*  
290 lipogenesis and lipid-associated macrophage recruitment in atherosclerotic liver, and thus  
291 decreased liver steatosis.

### 292 **Activin A decreased inflammatory gene expression**

293 We next explored how Activin A protects against inflammation. In overrepresentation analysis  
294 of DEG, “cytokine-cytokine receptor interaction” ranked 1 and “chemokine signaling pathway”  
295 ranked 4 among the KEGG pathways, and “cytokine-mediated signal pathway” ranked 2,  
296 “phagocytosis” ranked 5, “myeloid cell differentiation” ranked 10, and “leukocytes migration”  
297 ranked 11 among the GO Biological Process (Figure 4B and S3A). In addition, a heatmap  
298 generated for the DEG list from those pathways revealed downregulation of many genes involved

299 in leukocyte migration (GO) and cytokine-cytokine receptor interactions, such as  
300 monocyte/macrophage trafficking/migration chemokines CCL2 (also known as MCP1), CCL3,  
301 CCL4, CCL5, CCL6, CCL9<sup>59</sup>, macrophage markers CD68, CCR2 (the receptor of CCL2) and  
302 Lgals3, monocytes marker Ly-6C2, hepatic steatosis/ NASH associated lymphocyte antigen  
303 Ly6D, monocyte/macrophage homeostasis chemokine CXCL16, neutrophil trafficking chemokine  
304 CXCL1, as well as other pro-inflammatory chemokines CXCL9, CXCL10 and CXCL11 (Figure  
305 5A). Meanwhile, liver hematopoietic lineage markers, including CD44, CD48, Fcgr1 and Csf3r  
306 were decreased in Activin A-expressing mice compared with control (Figure 5A). Next, we  
307 confirmed by QPCR that the mRNA levels of all these genes were decreased in Activin A-  
308 expressing livers compared with controls (Figure 5B-5C). We performed flow cytometry on liver  
309 samples and found that Activin A expression leads to a ~50% decrease in F4/80+ macrophages,  
310 ~60% decrease in Ly-6C<sup>high</sup> monocytes, >50% decrease in PMN (polymorphonuclear cells), PMO  
311 (patrolling monocytes), as well as MDM (monocytes-derived macrophages) (Figure 5D-5G). In  
312 addition, eosinophils were also decreased in Activin A-expressing livers (Figure 5E, 5G).  
313 However, MM (mature macrophages or Kupffer cells) did not significantly change (Figure 5E,  
314 5G). These data suggest that Activin A expression decreased liver inflammation and recruitment  
315 of inflammatory monocytes/macrophages and PMNs to the liver.

### 316 **Activin A inhibits fat accumulation and improves glucose tolerance**

317 Cardiovascular diseases, including atherosclerosis, are highly correlated with obesity and  
318 diabetes<sup>60</sup>, and Activin A regulated genes *Scd1* may also play crucial roles in obesity and diabetes.  
319 This led us to probe whether Activin A affects WAT lipogenesis and glucose tolerance. H&E  
320 staining showed that Activin A led to ~2-fold decrease in epididymal, and inguinal WAT (Figure  
321 6A-6B). In addition, adipocyte size was dramatically decreased in epididymal and inguinal WAT)

322 by hepatic Activin A expression liver compared with controls (Figure 6A, 6C). Moreover, fasting  
323 glucose levels were substantially decreased by hepatic Activin A expression compared with  
324 controls (Figure 6D). Furthermore, Activin A expression in liver resulted in improved glucose  
325 tolerance (Figure 6E). Overall, these data demonstrate that hepatic Activin A inhibited fat  
326 accumulation and improved glucose tolerance in atherosclerotic mice.

327

## 328 **Discussion**

329 Here we report that Activin A exogenously expressed in the liver protects against  
330 atherosclerosis. AAV8-TBG-Activin A treatment resulted in a ~40% decrease in plasma LDL  
331 cholesterol, ~50% decrease in plasma total cholesterol, ~60% decrease in atherosclerotic lesions  
332 in the aortic arch, and fewer inflammatory cells infiltrating aortas and proliferating HSC in bone  
333 marrow. Hepatic Activin A not only reduced liver steatosis by inhibiting Srebp1 and Srebp2  
334 expression and hepatic *de novo* lipogenesis, as well as exogenous fatty acid uptake, but also  
335 alleviated liver inflammation and reduced monocytes, macrophages, and neutrophil infiltration. In  
336 addition, Activin A expression in liver also reduced white fat tissue accumulation and adipocyte  
337 size as well as improving glucose tolerance. Taken together these data suggest the reduction in  
338 hepatic Activin A observed in mice on the Western diet is maladaptive and demonstrate that  
339 hepatic Activin A expression has a host of favorable effects in this context that culminate in  
340 reduced atherosclerosis and hepatic steatosis, phenotypes that cause significant morbidity and  
341 mortality throughout the world.

342 Increased Activin A has previously been reported in vascular lesions and plasma of patients  
343 with atherosclerosis<sup>19</sup>, but whether it contributed to disease pathogenesis or played a compensatory  
344 protective role has not been firmly established. While plasma Activin A was indeed increased in

345 hyperlipidemic mice in our study, we observed a decrease in Activin A expression in the aorta and  
346 liver of these animals. Together with the finding that increasing Activin A in the liver and  
347 circulation attenuates the development of atherosclerosis, these observations suggest that the  
348 increase in Activin A reported in patient plasma and lesions may reflect a compensatory change.

349 While previous studies have identified anti-atherosclerotic effects of Activin A signaling on  
350 cellular processes within the vessel wall such as foam cell formation and vascular smooth muscle  
351 cell differentiation *in vitro*, our data suggest that important primary contributors to Activin's anti-  
352 atherosclerotic effects in the LDLR<sup>-/-</sup> murine model lie outside the vessel. In line with the dramatic  
353 decrease in plasma LDL and total cholesterol observed in Activin A-treated mice, our liver RNA-  
354 seq studies were consistent with anti-atherogenic changes in liver lipid metabolism, and reduced  
355 Srebp1 and Srebp2. Subsequent validation studies confirmed downregulation of key transcription  
356 factors and enzymes involved in cholesterol and triglyceride metabolism and fatty acid uptake  
357 (Srebp1 and Srebp2, Scd1/ Scd2, Fads2, Fabp1 and CD36) (Figure 6F), and reduced liver total  
358 cholesterol and free cholesterol. The reduction in cholesterol synthesis and fatty acid uptake likely  
359 contribute to the reduced inflammation seen in both the aorta and liver. Consistently, knockout of  
360 fatty acid desaturase (Fads2) reduces cholesterol and triglycerides and protects against Western  
361 diet-induced atherosclerosis<sup>61</sup>. In addition, bone marrow transplantation of HSC from Fabp5  
362 deficiency mice protects against atherosclerosis in LDLR<sup>-/-</sup> mice<sup>62</sup>. Here, Activin A had other  
363 beneficial effects including a reduction in proliferating HSCs, reduction in WAT, and improved  
364 glucose tolerance. Some of these effects may be secondary to the observed reduction in total and  
365 LDL cholesterol but other primary mechanisms may also be contributing and will be of interest  
366 for future studies.



367 In broad terms, many effects of Activin A (and other GDF/BMP proteins) can be seen as  
368 toggling tissues between catabolic and anabolic states. Throughout evolution in calorie scarce  
369 environments, downregulation of Activin may have been an adaptive response that conserved  
370 energy and activated useful anabolic processes. However, in calorie rich settings, exemplified  
371 here by the Western diet, the downregulation of Activin A appears maladaptive, promoting  
372 atherogenesis and hepatic steatosis, major causes of morbidity and mortality in the modern world.

373 Other members of the Activin/GDF/TGF $\beta$ /BMP family have also been reported to have roles  
374 in atherosclerosis. GDF11, another ligand for ACVR receptors, protected against atherosclerosis  
375 in ApoE<sup>-/-</sup> mice by ameliorating inflammation and endothelial cell injury<sup>63</sup>. Knockout of the  
376 TGF $\beta$  receptor, TGF $\beta$ RII, in dendritic cells, smooth muscle cells and T cell was reported to  
377 accelerate atherosclerosis while knockout of TGF $\beta$ RII in endothelial cells protected against  
378 atherosclerosis<sup>64-67</sup>. Neutralization of TGF $\beta$  with an antibody (anti-hTGF- $\beta$ 1, - $\beta$ 2, - $\beta$ 3 2G7  
379 monoclonal) increased atherosclerosis and inflammation<sup>68</sup>. Interestingly, TGF $\beta$ 1 was also reported  
380 to induce HSC quiescence and cell cycle arrest by upregulation of p57, a member of the cyclin-  
381 dependent kinase inhibitor family<sup>69, 70</sup>. Bone marrow transplantation studies showed that the  
382 hematopoietic stem/progenitor population was reduced in bone marrow from TGF $\beta$ 1KO pups and  
383 bone marrow reconstitution was impaired compared with TGF $\beta$ 1<sup>+/+</sup> pups<sup>71</sup>. However, TGF $\beta$ 1  
384 receptor I (TGF $\beta$ RI) deficient mice showed normal HSC self-renewal and regeneration ability<sup>72</sup>.  
385 This is partially because TGF $\beta$ 2, another isoform of TGF $\beta$ , supports LSK cell proliferation<sup>73</sup>. It  
386 will be interesting to probe the role of Activin A, its receptors, as well as other ligands in Activin  
387 pathway in HSC self-renewal, regeneration, expansion, and atherosclerosis.

388 Interestingly, we did not see pro-fibrotic or pro-apoptotic effects of hepatic Activin A  
389 expressions despite prior reports of such effects with other members of this protein family. Rather,

390 we instead saw a robust decrease in fibrosis markers and no alteration in apoptosis in the liver  
391 (data not shown) in hyperlipidemic mice treated with Activin A. Unlike the classic TGF $\beta$  signaling  
392 pathways, Activin A is regulated by a negative feedback loop. FST is not only a direct target but  
393 also a strong antagonist of these pathway. In addition, Activin A also forms a non-signaling  
394 complex with the type I receptors (ACVR1a, ALK2) and type II receptor. These self-limiting  
395 mechanisms may preserve homeostasis and prevent overactivation of the Activin A pathway. The  
396 expression level of Activin A is likely a key determinant of whether these self-limiting pathways  
397 are activated or not, with beneficial or harmful consequences for the liver. Here we delivered a  
398 very low dosage of AAV8-TBG-Activin A ( $2 \times 10^{10}$  genome copies/mice,  $\sim 2000$  pg/ml in plasma,  
399 compared to the common dose of  $1-2 \times 10^{11}$  genome copies/mouse<sup>32-34</sup>). This level of expression  
400 activated downstream signaling, as indicated by an increase in phosphorylation of Smad2/3, as  
401 well as increased FST. The Activin A receptors ACVR1b, ACVR2a, and ACVR2b were also  
402 decreased or showed a nonsignificant trend toward decrease. Interestingly, levels of the liver injury  
403 marker plasma ALT greatly decreased in Activin A expressing liver compared with control,  
404 suggesting a low dosage of AAV8-TBG-Activin A may be beneficial for the liver. This is  
405 consistent with a previous study showing low-dose AAV2/8-smad3 ( $2 \times 10^9$  genome copies/mice)  
406 attenuated aortic atherosclerosis without increasing fibrosis<sup>74</sup>.

407 The beneficial effects of hepatic Activin A expression raise the intriguing possibility that  
408 Activin A expression could have therapeutic potential. However, reasonable concerns could be  
409 raised about this approach. We have previously shown that Activin A levels increase with age in  
410 humans and contribute to multiple models of cardiac dysfunction and heart failure<sup>75</sup>. Activin A  
411 was sufficient to cause cardiac dysfunction in healthy mice but importantly, that was at higher  
412 concentrations of Activin A ( $\sim 10,000$  pg/ml) by adenovirus delivery without special diet<sup>75</sup>. Here,

413 the levels of Activin expression used were lower and echocardiography did not reveal alterations  
414 in cardiac function (data not shown). Still there could be legitimate concerns about therapeutic  
415 windows particularly given the challenges of fine-tuning concentrations achieved with gene  
416 therapy approaches. Finally, while the growing number of treatments available for primary and  
417 secondary prevention of atherosclerosis may undermine interest in that setting, no drugs have been  
418 approached for hepatic steatosis or the closely related non-alcoholic liver disease suggesting there  
419 may be greater enthusiasm for evaluation of Activin A's ability to address this important unmet  
420 clinical need.

421 Activin A also reduced WAT and improved glucose tolerance, suggesting a potential beneficial  
422 role for Activin A in obesity and diabetes, similar with hepatic Activin E<sup>76</sup>. However, this may  
423 seem paradoxical given that *deletion* of a closely related protein, myostatin (GDF8) has been  
424 shown to reduce obesity and protect against diabetes in mice<sup>77</sup>. It seems possible that deletion and  
425 overexpression could culminate in similar phenotypes through different mechanisms. For example,  
426 the dramatic skeletal muscle growth seen in myostatin knockout mice likely mediates multiple  
427 metabolic benefits while the catabolic state induced by overexpression of Activin A may reduce  
428 fat storage and insulin resistance. In this context, it would be interesting in future studies to  
429 examine the effects of genetic or pharmacological inhibition of these pathways in atherosclerosis  
430 as well.

431 In summary, the data presented here reveal for the first time that Activin A expressed in the  
432 liver protects against atherosclerosis, as well as liver steatosis and inflammation, reduces fat  
433 accumulation and improves glucose tolerance. These findings have implications for our  
434 understanding of the role of this pathway and the regulation of processes central to atherogenesis,  
435 while suggesting the therapeutic potential of moderate hepatic Activin A expression in

436 atherosclerotic vascular disease and hepatic disorders, such as obesity and non-alcoholic liver  
437 disease, warrants further investigation.

438

439 **Acknowledgments:** We acknowledge Suying Liu (Children’s Hospital of Philadelphia), Dr. Shun  
440 He and Dr. Alexandre Paccalet (Center for Systems Biology, MGH), Dr. Anlu Chen (Broad  
441 Institutes) for their technical supports and professional suggestions, Danian Cao (Wellman Center  
442 Photopathology Core, MGH) for flow cytometry analysis, Yoshiko Iwamoto (Center for Systems  
443 Biology, MGH) for tissue staining, and Photopathology Core Wellman Center, MGH CCM Clinic  
444 Pathology Lab, and MGH Histopathology Research Core for their services.

445 H.L, and A.R conceived this study. H.L designed and performed experiments, analyzed data,  
446 wrote, and edited the manuscript. M.H.H wrote and edited the manuscript. C.Y.X performed  
447 echocardiography. R.K. J.B.G, H.L, and A.K analyzed RNA-seq data. A.R supervised the study,  
448 analyzed data, wrote, and edited the manuscript, and secured funding.

449

450 **Sources of Funding:** This research is supported by the National Institutes of Health  
451 (R01AG061034, R35HL155318 to Dr Rosenzweig).

452

453 **Disclosures:** The authors declare that they have no conflicts of interest with the contents of this  
454 article.

455

## 456 **Supplemental Material**

457 Supplemental Materials and Methods

458 Supplemental Table 1

459 Supplemental Figure S1, S2, and S3

460 Supplemental References 29-31

461

462

## 463 References

- 464 1. <Hannah Ritchie and Max Roser (2018) - "Causes of Death". Published online at  
465 OurWorldInData.org. Retrieved from: '<https://ourworldindata.org/causes-of-death>' [Online  
466 Resource].
- 467 2. Gistera A, Hansson GK. The immunology of atherosclerosis. *Nat Rev Nephrol.* 2017;13:368-380
- 468 3. Swirski FK, Libby P, Aikawa E, Alcaide P, Luscinskas FW, Weissleder R, et al. Ly-6chi monocytes  
469 dominate hypercholesterolemia-associated monocytosis and give rise to macrophages in  
470 atheromata. *J Clin Invest.* 2007;117:195-205
- 471 4. Shiomi M, Ito T, Tsukada T, Yata T, Watanabe Y, Tsujita Y, et al. Reduction of serum cholesterol  
472 levels alters lesional composition of atherosclerotic plaques. Effect of pravastatin sodium on  
473 atherosclerosis in mature whhl rabbits. *Arterioscler Thromb Vasc Biol.* 1995;15:1938-1944
- 474 5. Abe RJ, Abe JI, Nguyen MTH, Olmsted-Davis EA, Mamun A, Banerjee P, et al. Free cholesterol  
475 bioavailability and atherosclerosis. *Curr Atheroscler Rep.* 2022;24:323-336
- 476 6. Li H, Yu XH, Ou X, Ouyang XP, Tang CK. Hepatic cholesterol transport and its role in non-alcoholic  
477 fatty liver disease and atherosclerosis. *Prog Lipid Res.* 2021;83:101109
- 478 7. Gluchowski NL, Becuwe M, Walther TC, Farese RV, Jr. Lipid droplets and liver disease: From basic  
479 biology to clinical implications. *Nat Rev Gastroenterol Hepatol.* 2017;14:343-355
- 480 8. Horton JD, Shimomura I, Brown MS, Hammer RE, Goldstein JL, Shimano H. Activation of  
481 cholesterol synthesis in preference to fatty acid synthesis in liver and adipose tissue of  
482 transgenic mice overproducing sterol regulatory element-binding protein-2. *J Clin Invest.*  
483 1998;101:2331-2339
- 484 9. Karasawa T, Takahashi A, Saito R, Sekiya M, Igarashi M, Iwasaki H, et al. Sterol regulatory  
485 element-binding protein-1 determines plasma remnant lipoproteins and accelerates  
486 atherosclerosis in low-density lipoprotein receptor-deficient mice. *Arterioscler Thromb Vasc Biol.*  
487 2011;31:1788-1795
- 488 10. Tang JJ, Li JG, Qi W, Qiu WW, Li PS, Li BL, et al. Inhibition of srebp by a small molecule, betulin,  
489 improves hyperlipidemia and insulin resistance and reduces atherosclerotic plaques. *Cell Metab.*  
490 2011;13:44-56
- 491 11. Yu H, Rimbert A, Palmer AE, Toyohara T, Xia Y, Xia F, et al. Gpr146 deficiency protects against  
492 hypercholesterolemia and atherosclerosis. *Cell.* 2019;179:1276-1288 e1214
- 493 12. Morianos I, Papadopoulou G, Semitekolou M, Xanthou G. Activin-a in the regulation of immunity  
494 in health and disease. *J Autoimmun.* 2019;104:102314
- 495 13. Yadin D, Knaus P, Mueller TD. Structural insights into bmp receptors: Specificity, activation and  
496 inhibition. *Cytokine Growth Factor Rev.* 2016;27:13-34
- 497 14. Thompson TB, Lerch TF, Cook RW, Woodruff TK, Jardetzky TS. The structure of the  
498 follistatin:Activin complex reveals antagonism of both type i and type ii receptor binding. *Dev*  
499 *Cell.* 2005;9:535-543
- 500 15. Blount AL, Vaughan JM, Vale WW, Bilezikjian LM. A smad-binding element in intron 1  
501 participates in activin-dependent regulation of the follistatin gene. *J Biol Chem.* 2008;283:7016-  
502 7026
- 503 16. Aykul S, Corpina RA, Goebel EJ, Cunanan CJ, Dimitriou A, Kim HJ, et al. Activin a forms a non-  
504 signaling complex with acvr1 and type ii activin/bmp receptors via its finger 2 tip loop. *Elife.*  
505 2020;9
- 506 17. Macias-Silva M, Hoodless PA, Tang SJ, Buchwald M, Wrana JL. Specific activation of smad1  
507 signaling pathways by the bmp7 type i receptor, alk2. *J Biol Chem.* 1998;273:25628-25636

- 508 18. Hatsell SJ, Idone V, Wolken DM, Huang L, Kim HJ, Wang L, et al. Acvr1r206h receptor mutation  
509 causes fibrodysplasia ossificans progressiva by imparting responsiveness to activin a. *Sci Transl*  
510 *Med.* 2015;7:303ra137
- 511 19. Engelse MA, Neele JM, van Achterberg TA, van Aken BE, van Schaik RH, Pannekoek H, et al.  
512 Human activin-a is expressed in the atherosclerotic lesion and promotes the contractile  
513 phenotype of smooth muscle cells. *Circ Res.* 1999;85:931-939
- 514 20. Oklu R, Hesketh R, Wicky S, Metcalfe J. Tgfbeta/activin signaling pathway activation in intimal  
515 hyperplasia and atherosclerosis. *Diagn Interv Radiol.* 2011;17:290-296
- 516 21. Smith C, Yndestad A, Halvorsen B, Ueland T, Waehre T, Otterdal K, et al. Potential anti-  
517 inflammatory role of activin a in acute coronary syndromes. *J Am Coll Cardiol.* 2004;44:369-375
- 518 22. Moore KJ, Tabas I. Macrophages in the pathogenesis of atherosclerosis. *Cell.* 2011;145:341-355
- 519 23. Kojima Y, Weissman IL, Leeper NJ. The role of efferocytosis in atherosclerosis. *Circulation.*  
520 2017;135:476-489
- 521 24. Kozaki K, Akishita M, Eto M, Yoshizumi M, Toba K, Inoue S, et al. Role of activin-a and follistatin  
522 in foam cell formation of thp-1 macrophages. *Arterioscler Thromb Vasc Biol.* 1997;17:2389-2394
- 523 25. Wang H, Zhang P, Chen X, Liu W, Fu Z, Liu M. Activin a inhibits foam cell formation and up-  
524 regulates abca1 and abcg1 expression through alk4-smad signaling pathway in raw 264.7  
525 macrophages. *Steroids.* 2021;174:108887
- 526 26. Engelse MA, Lardenoye JH, Neele JM, Grimbergen JM, De Vries MR, Lamfers ML, et al.  
527 Adenoviral activin a expression prevents intimal hyperplasia in human and murine blood vessels  
528 by maintaining the contractile smooth muscle cell phenotype. *Circ Res.* 2002;90:1128-1134
- 529 27. Yan Z, Yan H, Ou H. Human thyroxine binding globulin (tbg) promoter directs efficient and  
530 sustaining transgene expression in liver-specific pattern. *Gene.* 2012;506:289-294
- 531 28. Kimura T, Ferran B, Tsukahara Y, Shang Q, Desai S, Fedoce A, et al. Production of adeno-  
532 associated virus vectors for in vitro and in vivo applications. *Sci Rep.* 2019;9:13601
- 533 29. Wang X, Xu BL, Chen XW. Acute gene inactivation in the adult mouse liver using the crispr-cas9  
534 technology. *STAR Protoc.* 2021;2:100611
- 535 30. McAlpine CS, Kiss MG, Rattik S, He S, Vassalli A, Valet C, et al. Sleep modulates haematopoiesis  
536 and protects against atherosclerosis. *Nature.* 2019;566:383-387
- 537 31. Stijlemans B, Sparkes A, Abels C, Keirsse J, Brys L, Elkrim Y, et al. Murine liver myeloid cell  
538 isolation protocol. *Bio-protocol.* 2015;5:e1471
- 539 32. Zhao H, Li Y, He L, Pu W, Yu W, Li Y, et al. In vivo aav-crispr/cas9-mediated gene editing  
540 ameliorates atherosclerosis in familial hypercholesterolemia. *Circulation.* 2020;141:67-79
- 541 33. Wang X, Cai B, Yang X, Sonubi OO, Zheng Z, Ramakrishnan R, et al. Cholesterol stabilizes taz in  
542 hepatocytes to promote experimental non-alcoholic steatohepatitis. *Cell Metab.* 2020;31:969-  
543 986 e967
- 544 34. Ran FA, Cong L, Yan WX, Scott DA, Gootenberg JS, Kriz AJ, et al. In vivo genome editing using  
545 staphylococcus aureus cas9. *Nature.* 2015;520:186-191
- 546 35. King KY, Goodell MA. Inflammatory modulation of hscs: Viewing the hsc as a foundation for the  
547 immune response. *Nat Rev Immunol.* 2011;11:685-692
- 548 36. Wang LD, Wagers AJ. Dynamic niches in the origination and differentiation of haematopoietic  
549 stem cells. *Nat Rev Mol Cell Biol.* 2011;12:643-655
- 550 37. Teratani T, Tomita K, Suzuki T, Furuhashi H, Irie R, Hida S, et al. Free cholesterol accumulation in  
551 liver sinusoidal endothelial cells exacerbates acetaminophen hepatotoxicity via tlr9 signaling. *J*  
552 *Hepatol.* 2017;67:780-790
- 553 38. Teratani T, Tomita K, Suzuki T, Oshikawa T, Yokoyama H, Shimamura K, et al. A high-cholesterol  
554 diet exacerbates liver fibrosis in mice via accumulation of free cholesterol in hepatic stellate  
555 cells. *Gastroenterology.* 2012;142:152-164 e110

- 556 39. Ioannou GN. The role of cholesterol in the pathogenesis of nash. *Trends Endocrinol Metab.*  
557 2016;27:84-95
- 558 40. Horn CL, Morales AL, Savard C, Farrell GC, Ioannou GN. Role of cholesterol-associated  
559 steatohepatitis in the development of nash. *Hepatol Commun.* 2022;6:12-35
- 560 41. Iizuka K, Takao K, Yabe D. Chrebp-mediated regulation of lipid metabolism: Involvement of the  
561 gut microbiota, liver, and adipose tissue. *Front Endocrinol (Lausanne).* 2020;11:587189
- 562 42. Nakamura MT, Nara TY. Structure, function, and dietary regulation of delta6, delta5, and delta9  
563 desaturases. *Annu Rev Nutr.* 2004;24:345-376
- 564 43. Tabor DE, Kim JB, Spiegelman BM, Edwards PA. Identification of conserved cis-elements and  
565 transcription factors required for sterol-regulated transcription of stearoyl-coa desaturase 1 and  
566 2. *J Biol Chem.* 1999;274:20603-20610
- 567 44. Li B, Hao J, Zeng J, Sauter ER. Snapshot: Fabp functions. *Cell.* 2020;182:1066-1066 e1061
- 568 45. Chen A, Tang Y, Davis V, Hsu FF, Kennedy SM, Song H, et al. Liver fatty acid binding protein (I-  
569 fabp) modulates murine stellate cell activation and diet-induced nonalcoholic fatty liver disease.  
570 *Hepatology.* 2013;57:2202-2212
- 571 46. Febbraio M, Guy E, Silverstein RL. Stem cell transplantation reveals that absence of macrophage  
572 cd36 is protective against atherosclerosis. *Arterioscler Thromb Vasc Biol.* 2004;24:2333-2338
- 573 47. Hajri T, Han XX, Bonen A, Abumrad NA. Defective fatty acid uptake modulates insulin  
574 responsiveness and metabolic responses to diet in cd36-null mice. *J Clin Invest.* 2002;109:1381-  
575 1389
- 576 48. de Jager SC, Bermudez B, Bot I, Koenen RR, Bot M, Kavelaars A, et al. Growth differentiation  
577 factor 15 deficiency protects against atherosclerosis by attenuating ccr2-mediated macrophage  
578 chemotaxis. *J Exp Med.* 2011;208:217-225
- 579 49. Wang J, Wei L, Yang X, Zhong J. Roles of growth differentiation factor 15 in atherosclerosis and  
580 coronary artery disease. *J Am Heart Assoc.* 2019;8:e012826
- 581 50. Wang XA, Zhang R, Zhang S, Deng S, Jiang D, Zhong J, et al. Interferon regulatory factor 7  
582 deficiency prevents diet-induced obesity and insulin resistance. *Am J Physiol Endocrinol Metab.*  
583 2013;305:E485-495
- 584 51. Guzik TJ, West NE, Black E, McDonald D, Ratnatunga C, Pillai R, et al. Functional effect of the  
585 c242t polymorphism in the nad(p)h oxidase p22phox gene on vascular superoxide production in  
586 atherosclerosis. *Circulation.* 2000;102:1744-1747
- 587 52. Li JM, Newburger PE, Gounis MJ, Dargon P, Zhang X, Messina LM. Local arterial nanoparticle  
588 delivery of sirna for nox2 knockdown to prevent restenosis in an atherosclerotic rat model. *Gene*  
589 *Ther.* 2010;17:1279-1287
- 590 53. Martin-Ventura JL, Blanco-Colio LM, Munoz-Garcia B, Gomez-Hernandez A, Arribas A, Ortega L,  
591 et al. Nf-kappab activation and fas ligand overexpression in blood and plaques of patients with  
592 carotid atherosclerosis: Potential implication in plaque instability. *Stroke.* 2004;35:458-463
- 593 54. Item F, Wueest S, Lemos V, Stein S, Lucchini FC, Denzler R, et al. Fas cell surface death receptor  
594 controls hepatic lipid metabolism by regulating mitochondrial function. *Nat Commun.*  
595 2017;8:480
- 596 55. Cybulsky MI, Iiyama K, Li H, Zhu S, Chen M, Iiyama M, et al. A major role for vcam-1, but not  
597 icam-1, in early atherosclerosis. *J Clin Invest.* 2001;107:1255-1262
- 598 56. Lee GL, Yeh CC, Wu JY, Lin HC, Wang YF, Kuo YY, et al. Tlr2 promotes vascular smooth muscle cell  
599 chondrogenic differentiation and consequent calcification via the concerted actions of  
600 osteoprotegerin suppression and il-6-mediated rankl induction. *Arterioscler Thromb Vasc Biol.*  
601 2019;39:432-445

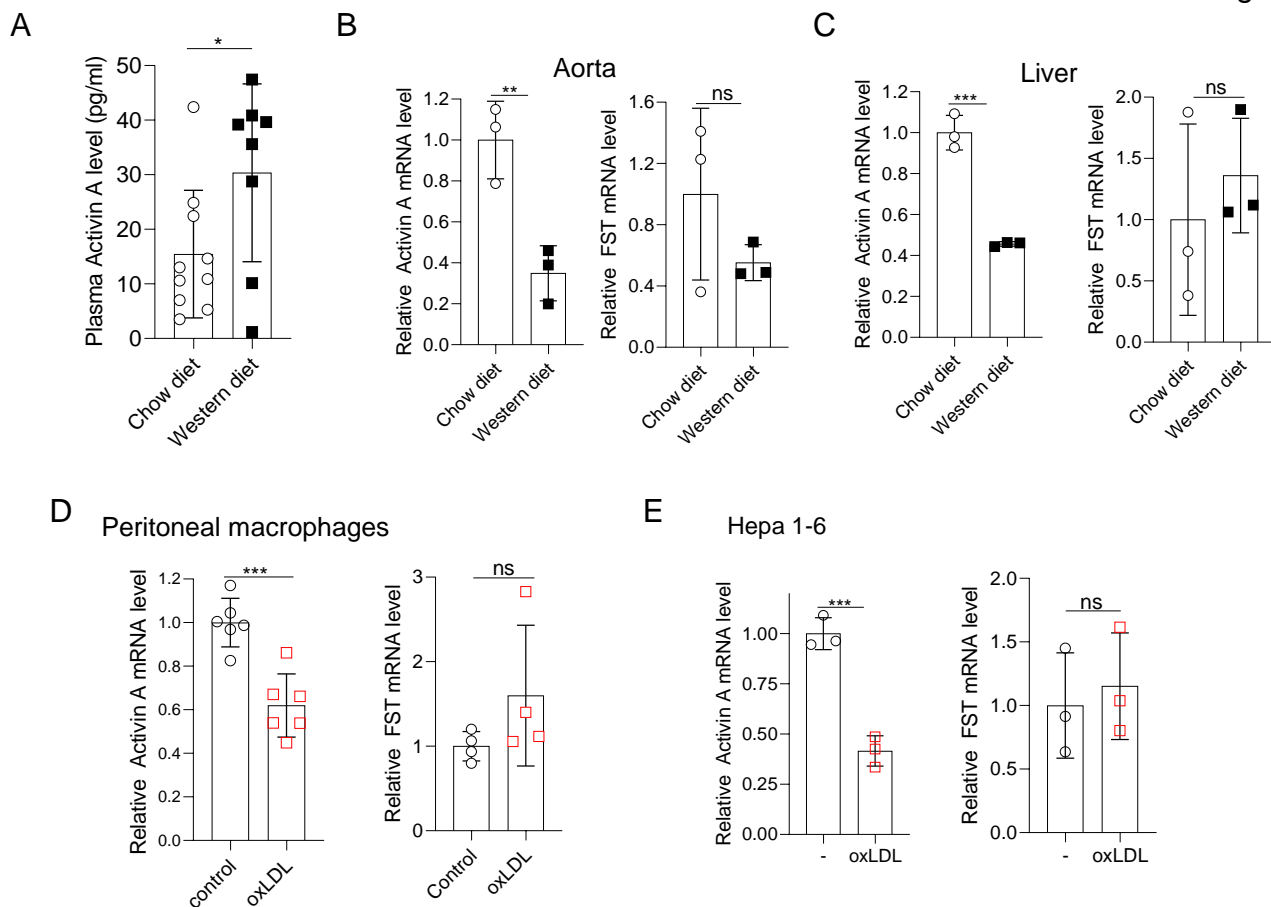


- 602 57. Gong XM, Li YF, Luo J, Wang JQ, Wei J, Wang JQ, et al. GpnmB secreted from liver promotes  
603 lipogenesis in white adipose tissue and aggravates obesity and insulin resistance. *Nat Metab.*  
604 2019;1:570-583
- 605 58. Xiong X, Kuang H, Ansari S, Liu T, Gong J, Wang S, et al. Landscape of intercellular crosstalk in  
606 healthy and nash liver revealed by single-cell secretome gene analysis. *Mol Cell.* 2019;75:644-  
607 660 e645
- 608 59. Cao S, Liu M, Sehrawat TS, Shah VH. Regulation and functional roles of chemokines in liver  
609 diseases. *Nat Rev Gastroenterol Hepatol.* 2021;18:630-647
- 610 60. Tokgozoglul, Libby P. The dawn of a new era of targeted lipid-lowering therapies. *Eur Heart J.*  
611 2022
- 612 61. Stoffel W, Binczek E, Schmidt-Soltau I, Brodesser S, Wegner I. High fat / high cholesterol diet  
613 does not provoke atherosclerosis in the omega3-and omega6-polyunsaturated fatty acid  
614 synthesis-inactivated delta6-fatty acid desaturase-deficient mouse. *Mol Metab.* 2021;54:101335
- 615 62. Babaev VR, Runner RP, Fan D, Ding L, Zhang Y, Tao H, et al. Macrophage mal1 deficiency  
616 suppresses atherosclerosis in low-density lipoprotein receptor-null mice by activating  
617 peroxisome proliferator-activated receptor-gamma-regulated genes. *Arterioscler Thromb Vasc*  
618 *Biol.* 2011;31:1283-1290
- 619 63. Mei W, Xiang G, Li Y, Li H, Xiang L, Lu J, et al. Gdf11 protects against endothelial injury and  
620 reduces atherosclerotic lesion formation in apolipoprotein e-null mice. *Mol Ther.* 2016;24:1926-  
621 1938
- 622 64. Chen PY, Qin L, Li G, Malagon-Lopez J, Wang Z, Bergaya S, et al. Smooth muscle cell  
623 reprogramming in aortic aneurysms. *Cell Stem Cell.* 2020;26:542-557 e511
- 624 65. Chen PY, Qin L, Li G, Wang Z, Dahlman JE, Malagon-Lopez J, et al. Endothelial tgf-beta signalling  
625 drives vascular inflammation and atherosclerosis. *Nat Metab.* 2019;1:912-926
- 626 66. Robertson AK, Rudling M, Zhou X, Gorelik L, Flavell RA, Hansson GK. Disruption of tgf-beta  
627 signaling in t cells accelerates atherosclerosis. *J Clin Invest.* 2003;112:1342-1350
- 628 67. Lievens D, Habets KL, Robertson AK, Laouar Y, Winkels H, Rademakers T, et al. Abrogated  
629 transforming growth factor beta receptor ii (tgfbetarii) signalling in dendritic cells promotes  
630 immune reactivity of t cells resulting in enhanced atherosclerosis. *Eur Heart J.* 2013;34:3717-  
631 3727
- 632 68. Mallat Z, Gojova A, Marchiol-Fournigault C, Esposito B, Kamate C, Merval R, et al. Inhibition of  
633 transforming growth factor-beta signaling accelerates atherosclerosis and induces an unstable  
634 plaque phenotype in mice. *Circ Res.* 2001;89:930-934
- 635 69. Scandura JM, Boccuni P, Massagué J, Nimer SD. Transforming growth factor beta-induced cell  
636 cycle arrest of human hematopoietic cells requires p57kip2 up-regulation. *Proc Natl Acad Sci U S*  
637 *A.* 2004;101:15231-15236
- 638 70. Blank U, Karlsson S. Tgf-beta signaling in the control of hematopoietic stem cells. *Blood.*  
639 2015;125:3542-3550
- 640 71. Capron C, Lacout C, Lecluse Y, Jalbert V, Chagraoui H, Charrier S, et al. A major role of tgf-beta1  
641 in the homing capacities of murine hematopoietic stem cell/progenitors. *Blood.* 2010;116:1244-  
642 1253
- 643 72. Larsson J, Blank U, Helgadottir H, Bjornsson JM, Ehinger M, Goumans MJ, et al. Tgf-beta  
644 signaling-deficient hematopoietic stem cells have normal self-renewal and regenerative ability in  
645 vivo despite increased proliferative capacity in vitro. *Blood.* 2003;102:3129-3135
- 646 73. Langer JC, Henckaerts E, Orenstein J, Snoeck HW. Quantitative trait analysis reveals  
647 transforming growth factor-beta2 as a positive regulator of early hematopoietic progenitor and  
648 stem cell function. *J Exp Med.* 2004;199:5-14

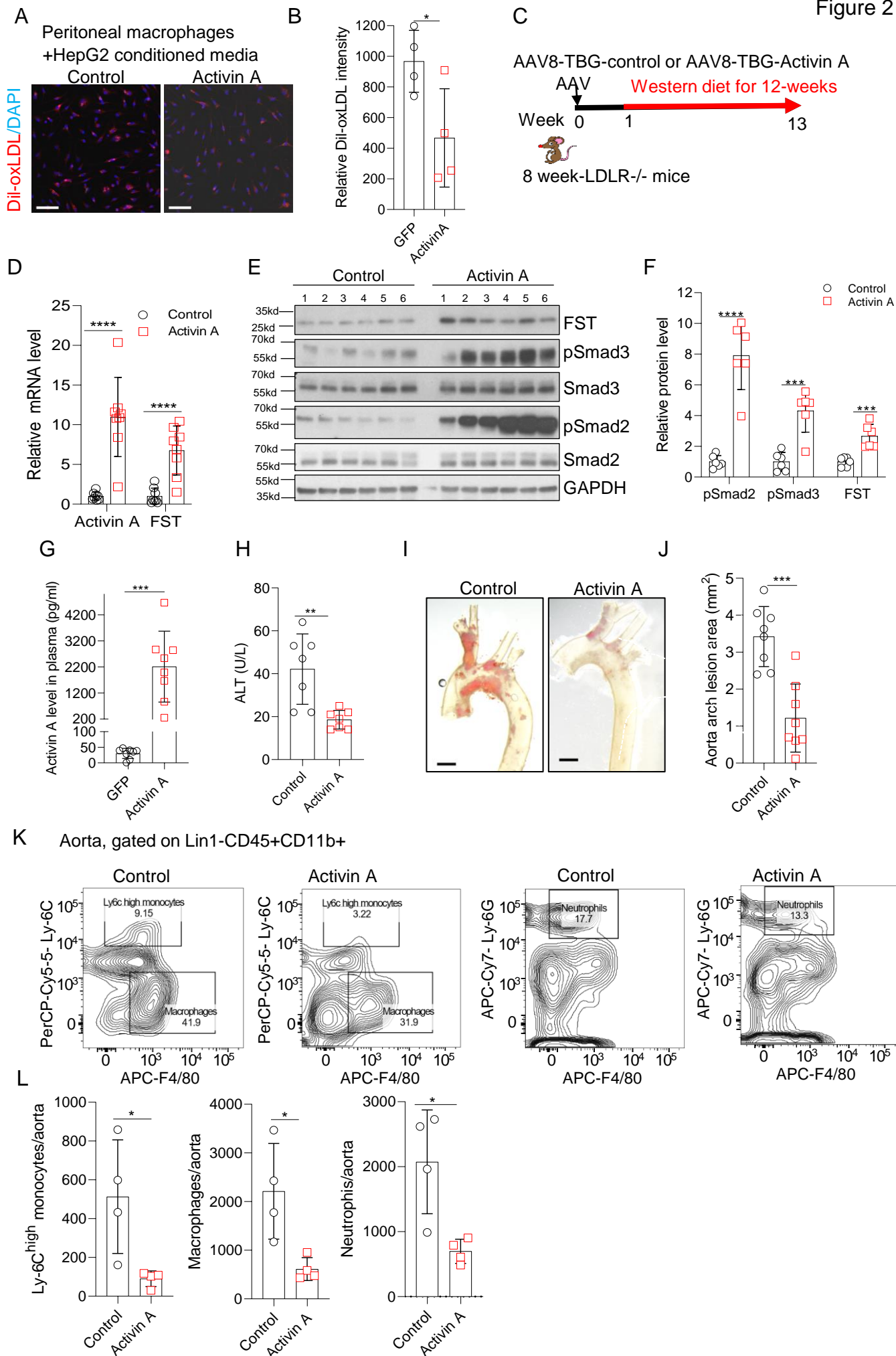
- 649 74. Zhu H, Cao M, Figueroa JA, Cobos E, Uretsky BF, Chiriva-Internati M, et al. Aav2/8-hsmad3 gene  
650 delivery attenuates aortic atherogenesis, enhances th2 response without fibrosis, in ldlr-ko mice  
651 on high cholesterol diet. *J Transl Med.* 2014;12:252
- 652 75. Roh JD, Hobson R, Chaudhari V, Quintero P, Yeri A, Benson M, et al. Activin type ii receptor  
653 signaling in cardiac aging and heart failure. *Sci Transl Med.* 2019;11
- 654 76. Hashimoto O, Funaba M, Sekiyama K, Doi S, Shindo D, Satoh R, et al. Activin e controls energy  
655 homeostasis in both brown and white adipose tissues as a hepatokine. *Cell Rep.* 2018;25:1193-  
656 1203
- 657 77. McPherron AC, Lee SJ. Suppression of body fat accumulation in myostatin-deficient mice.  
658 *Journal Of Clinical Investigation.* 2002;109:595-601

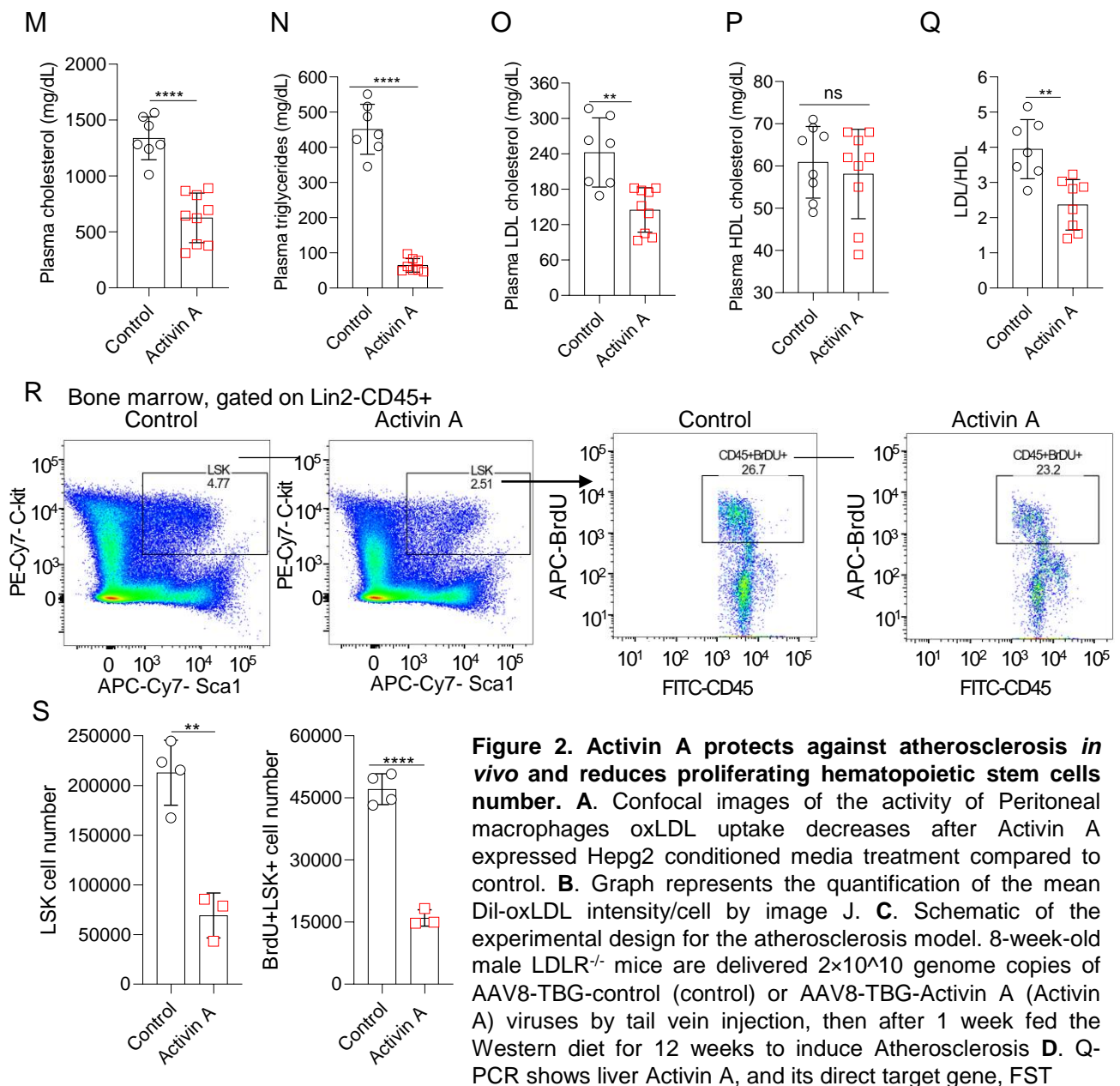
659

660



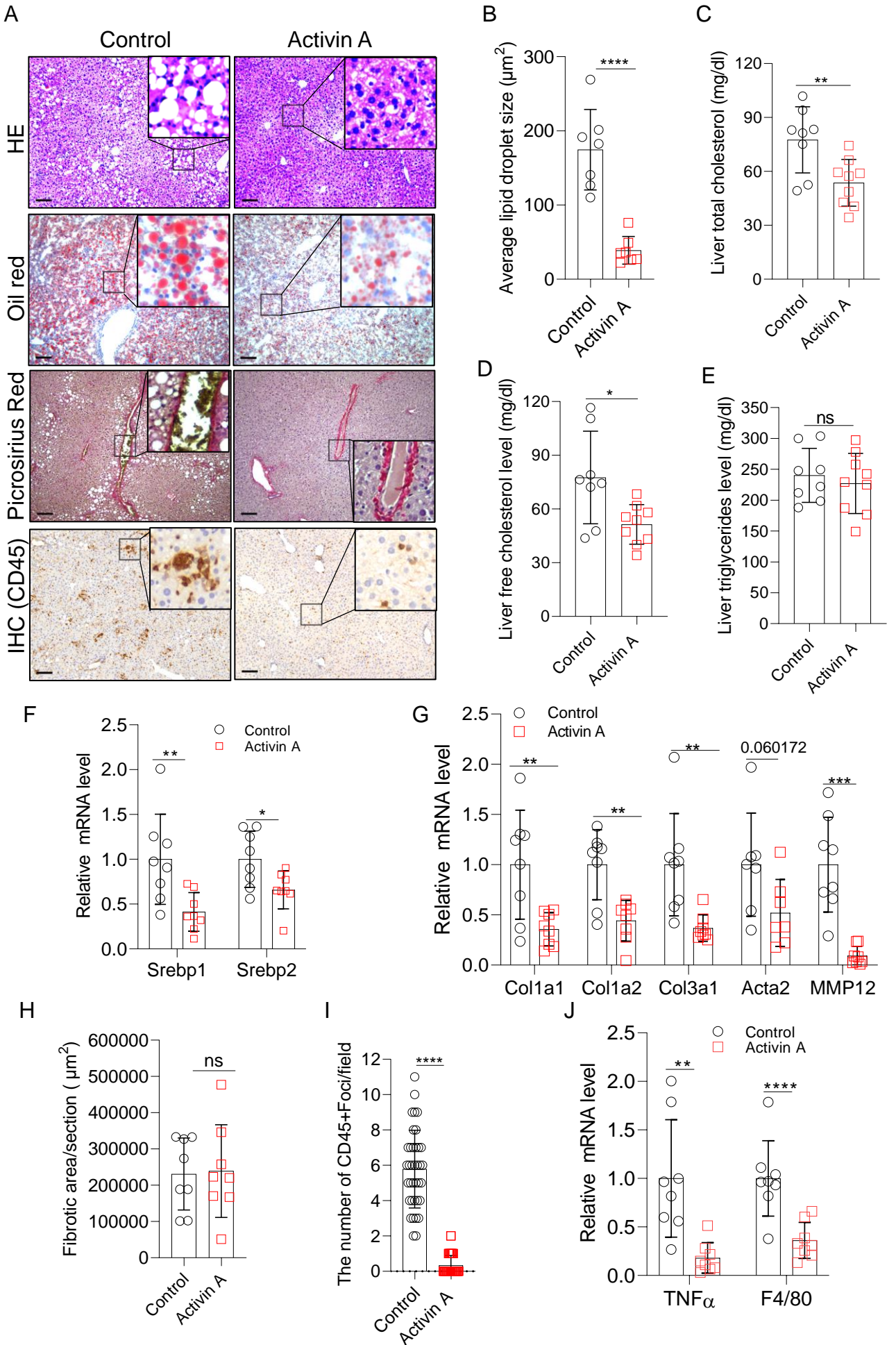
**Figure 1. Activin A mRNA decreases in aorta and liver in western diet fed mice, oxLDL treated macrophages and Hepa 1-6 cells.** **A.** ELISA shows plasma Activin A level in LDLR<sup>-/-</sup> mice fed with western diet for 12 weeks compared to chow diet. Plasma FST levels are close to baseline (0) and not shown here. N=8-10 mice. **B-C.** Q-PCR shows the Activin A but not FST mRNA decreases in the aorta and liver in LDLR<sup>-/-</sup> mice fed the western diet for 12 weeks compared to chow diet. N=3 mice. **D.** Q-PCR shows Activin A but not FST mRNA decreases in peritoneal macrophages after oxLDL treatment. Peritoneal macrophages were treated with and without 10µg/ml oxLDL in 0.5%BSA (fatty acid free)/RPMI at 37°C for 24h. **E.** Q-PCR shows Activin A but not FST mRNA decreased in oxLDL treated Hepa 1-6 cells. Hepa 1-6 cells were treated with and without 10 µg/ml oxLDL in 0.5%BSA (fatty acid free)/RPMI 1640 at 37°C for 24h.



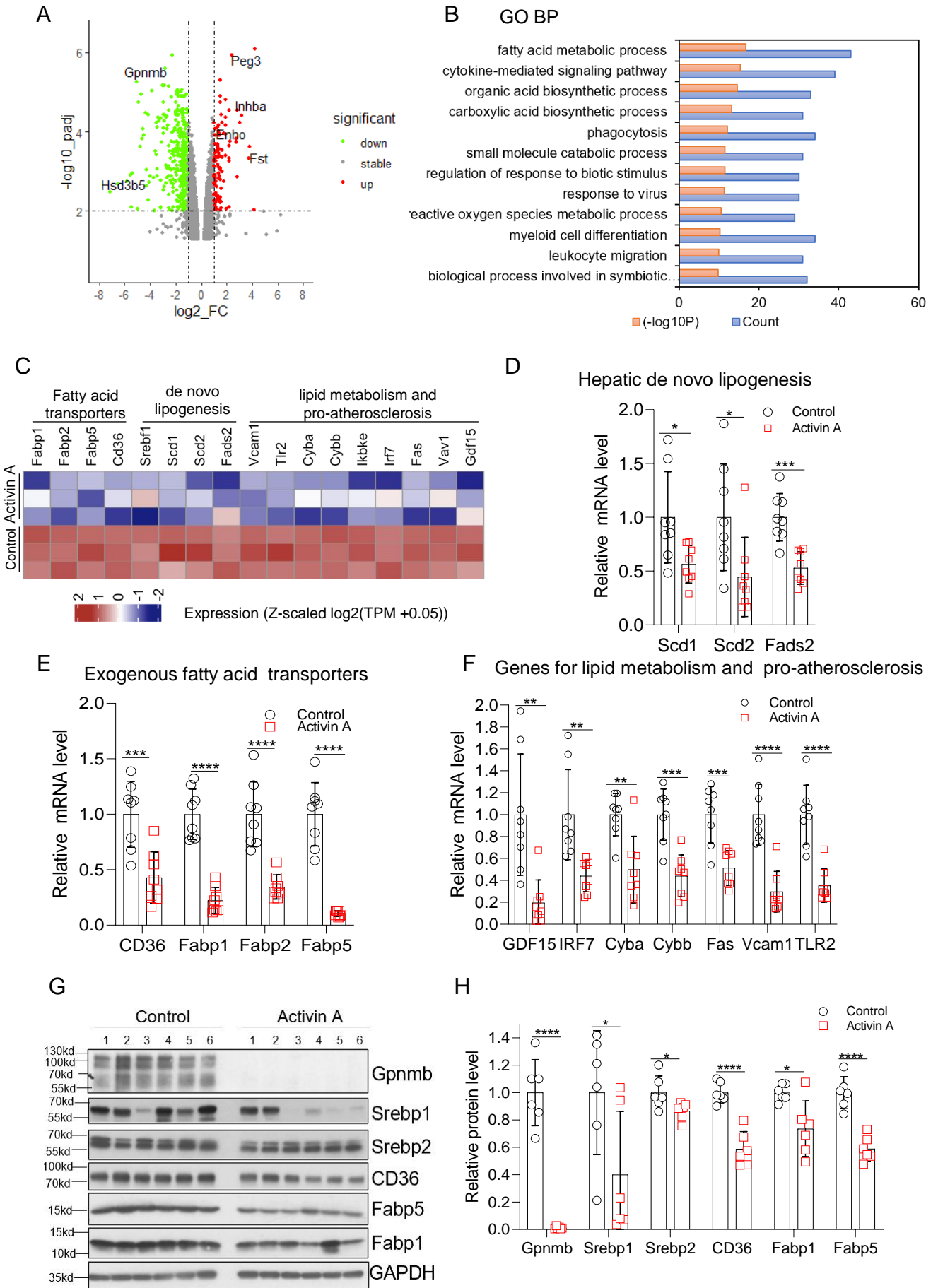


**Figure 2. Activin A protects against atherosclerosis *in vivo* and reduces proliferating hematopoietic stem cells number.** **A.** Confocal images of the activity of Peritoneal macrophages oxLDL uptake decreases after Activin A expressed Hepg2 conditioned media treatment compared to control. **B.** Graph represents the quantification of the mean Dil-oxLDL intensity/cell by image J. **C.** Schematic of the experimental design for the atherosclerosis model. 8-week-old male LDLR<sup>-/-</sup> mice are delivered 2×10<sup>10</sup> genome copies of AAV8-TBG-control (control) or AAV8-TBG-Activin A (Activin A) viruses by tail vein injection, then after 1 week fed the Western diet for 12 weeks to induce Atherosclerosis **D.** Q-PCR shows liver Activin A, and its direct target gene, FST

mRNA were induced in Activin A treated atherosclerotic LDLR<sup>-/-</sup> mice compared with control. N=8 mice. **E.** Western blotting shows the Activin signaling pathway is activated in Activin A expressing liver compared with control. Antibodies for Smad2, pSmad2, Smad3, pSmad3 and the Activin signaling pathway direct target gene FST were used, and GAPDH as the loading control. **F.** Quantification of relative pSmad2, pSmad3, and FST protein level. **G.** ELISA shows Activin A protein circulating in the plasma of atherosclerotic LDLR<sup>-/-</sup> mice after AAV8-TBG-Activin A treated and western diet for 12 weeks. N=8 mice. **H.** Graph represents plasma ALT (SGPT) decreases in Activin A treated atherosclerotic mice compared with control. **I.** Images show the oil red staining of atherosclerotic plaques in the aortic arch in control and Activin A expressing atherosclerotic mice. Scale bar, 1mm. **J.** Quantification of lesion area in the aortic arch. N=8 mice. **K.** Assessment and gating strategy of aortic immune cells by flow cytometry. Lin1: Ter119/NK1.1/CD19/CD90.2/CD3. Ly-6C<sup>high</sup> monocytes (CD45+Lin1-CD11b+F4/80-Ly-6C<sup>high</sup>), macrophages (CD45+Lin1-CD11b+F4/80+Ly-6C<sup>low</sup>) and neutrophils (CD45+Lin1-CD11b+Ly-6G+F4/80-). **L.** Quantification of Ly-6C<sup>high</sup> monocytes, macrophages, and neutrophils in aorta. N=4 mice. **M-Q.** Graphs represent the plasma lipid profiles including cholesterol, triglycerides, LDL, HDL and LDL/HDL in control and Activin A-expressing atherosclerotic mice. N=7-9 mice. **R.** Assessment and gating strategy of hematopoietic stem cells (HSC) proliferation by flow cytometry. Lin2: CD3/Ly-6G/Ly-6C/ B220/CD11B/Ter119/CD127. LSK: Lin2-CD45+Sca1+c-Kit+. **S.** Quantification of the of LSK cells and BrdU+ LSK cells. HSC were from 2 tibia and 2 femurs of each atherosclerotic mouse. 1mg BrdU was injected into mice 2 hours before euthanasia. N=3-4 mice. Similar results were obtained from 3 independent experiments.



**Figure 3. Activin A decreases liver steatosis and inflammation in atherosclerotic mice. A.** Representative Hematoxylin and Eosin staining, oil red staining (lipid), picosirius red staining (collagen I and III), and immunohistochemistry staining of leukocytes (with anti-CD45 antibody) in liver samples from control and Activin A treated –atherosclerotic mice. N=7-8 mice in each staining. **B.** Quantitation of the lipid droplet size based on oil red staining in A. N=8 mice. **C-E.** Graph represent the liver total cholesterol, free cholesterol level and triglycerides in atherosclerotic mice. N=7-9 mice. **F.** Q-PCR showing the mRNA level of Srebp1 and Srebp2, the key transcription factors for cholesterol synthesis and triglycerides in control and Activin A- expressing liver. N=8 mice. **G.** Q-PCR showing the mRNA level of fibrosis marker genes (Col1a1, Col1a2, Col3a1 and MMP12) and hepatic stellate cell marker gene (Acta2) in control and Activin A-expressing liver. N=8 mice. **H.** Quantification of fibrotic area of in the right lateral lobe based on picosirius red staining in A. N=8 mice. **I.** Quantification of CD45+ foci based on IHC staining in A. CD45+ foci was defined as the sites with > 8 CD45 positive cells. The number of CD45+ foci/field (7-8 field/mice) in the right lateral lobe was quantified. N=8 mice. **J.** Q-PCR showing the mRNA level of inflammatory marker genes  $TNF\alpha$ , and F4/80 in control and Activin A expressing- atherosclerotic liver. N=8 mice. Mean values for each mouse were used for quantification.





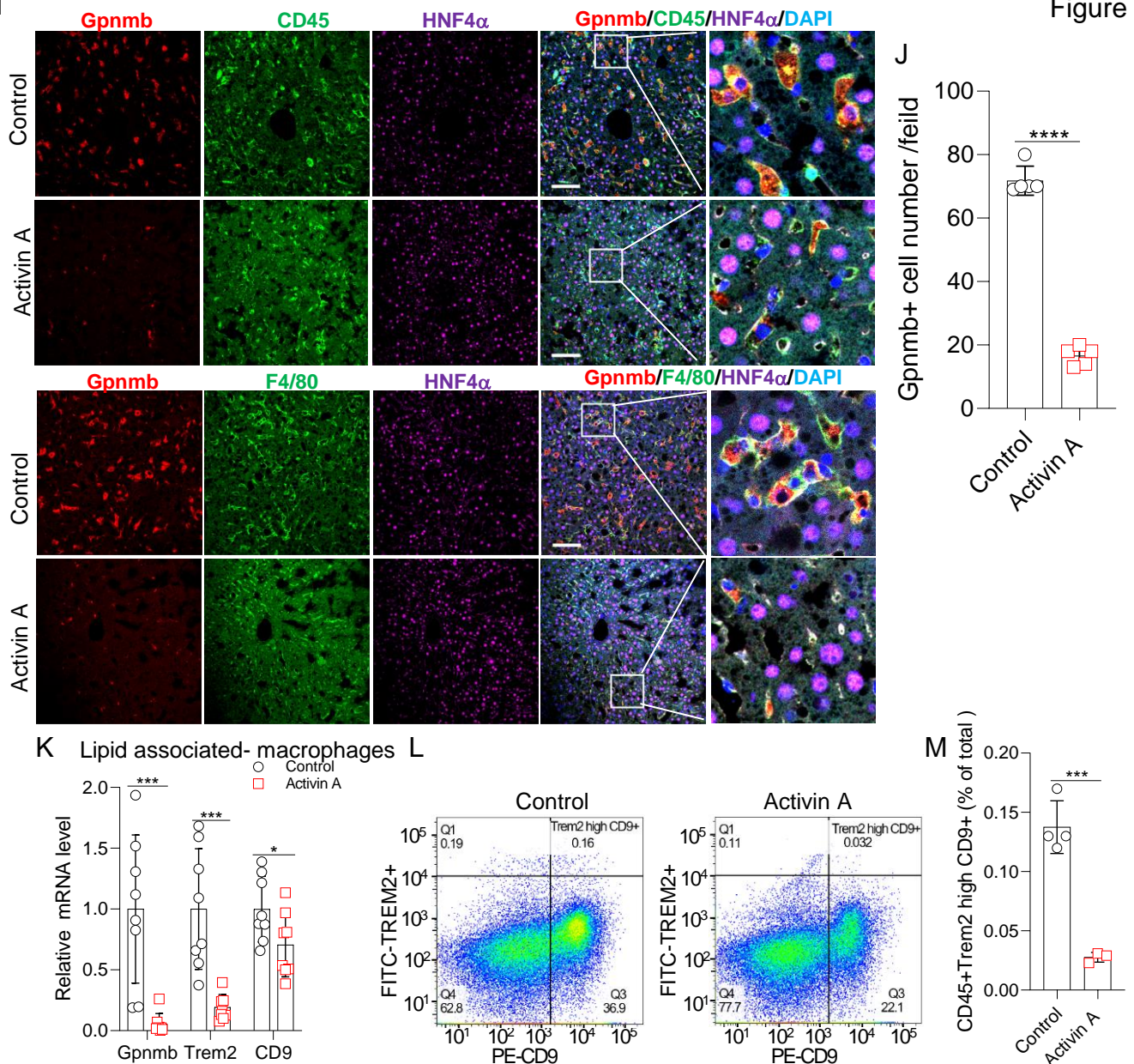


**Figure 4. Activin A decreases expression of genes involved in fatty acid uptake, and *de novo* lipogenesis, and lipid associated- macrophage markers in atherosclerotic liver.**

**A.** Representative volcano plot of differentially regulated genes in RNA-seq analysis of Activin A expressed liver compared with control. Triplicates per group. TPM (control) or TPM (Activin A)  $\geq 5$ . Significant:  $|\log_2 F_c| \geq 1$ ,  $p_{adj} < 0.01$ .

Downregulation: green, upregulation: red, and stable: grey. Labeling genes,  $p_{adj} < 0.01$ ,  $TPM \geq 10$ ,  $\log_2 F_c \geq 3$  or  $\log_2 F_c \leq -5$ .

**B.** Top 12 GO biological processes dramatically changed in RNA-seq analysis of Activin A-expressing liver compared with control, based on overrepresentation analysis. Cluster Profiles package was used. TPM (control) or TPM (Activin A)  $\geq 5$ ,  $p < 0.05$ ,  $|\log_2 F_c| \geq 1$ .

**C.** Heatmap shows differentially regulated featured genes in fatty acid metabolic process, lipid metabolism and atherosclerosis. Gene list is from GO and KEGG enrichment. TPM (control) or TPM (Activin A)  $\geq 5$ ,  $p < 0.05$ ,  $|\log_2 F_c| \geq 1$ ,  $p_{adj} < 0.01$ . Relative gene expression values (Z-scaled  $\log_2(TPM + 0.05)$ ) were represented.

**D-E.** Q-PCR confirmation of decreased transcript expression of genes involved in hepatic *de novo* lipogenesis and exogenous fatty acid uptake in Activin A-expressing liver compared with control. N=8 mice.

**F.** Q-PCR confirmation of decreased transcript expression of genes involved in lipid metabolism and atherosclerosis in Activin A expressing liver compared with control. N=8 mice.

**G.** Western blotting showing decreased Gpnmb, Srebp1, Srebp2, CD36, Fabp1, Fabp5 protein in Activin A-expressing liver compared with control. Antibodies for Gpnmb, Srebp1, Srebp2, CD36, Fabp1, and Fabp5 antibodies were used, GAPDH as the loading control.

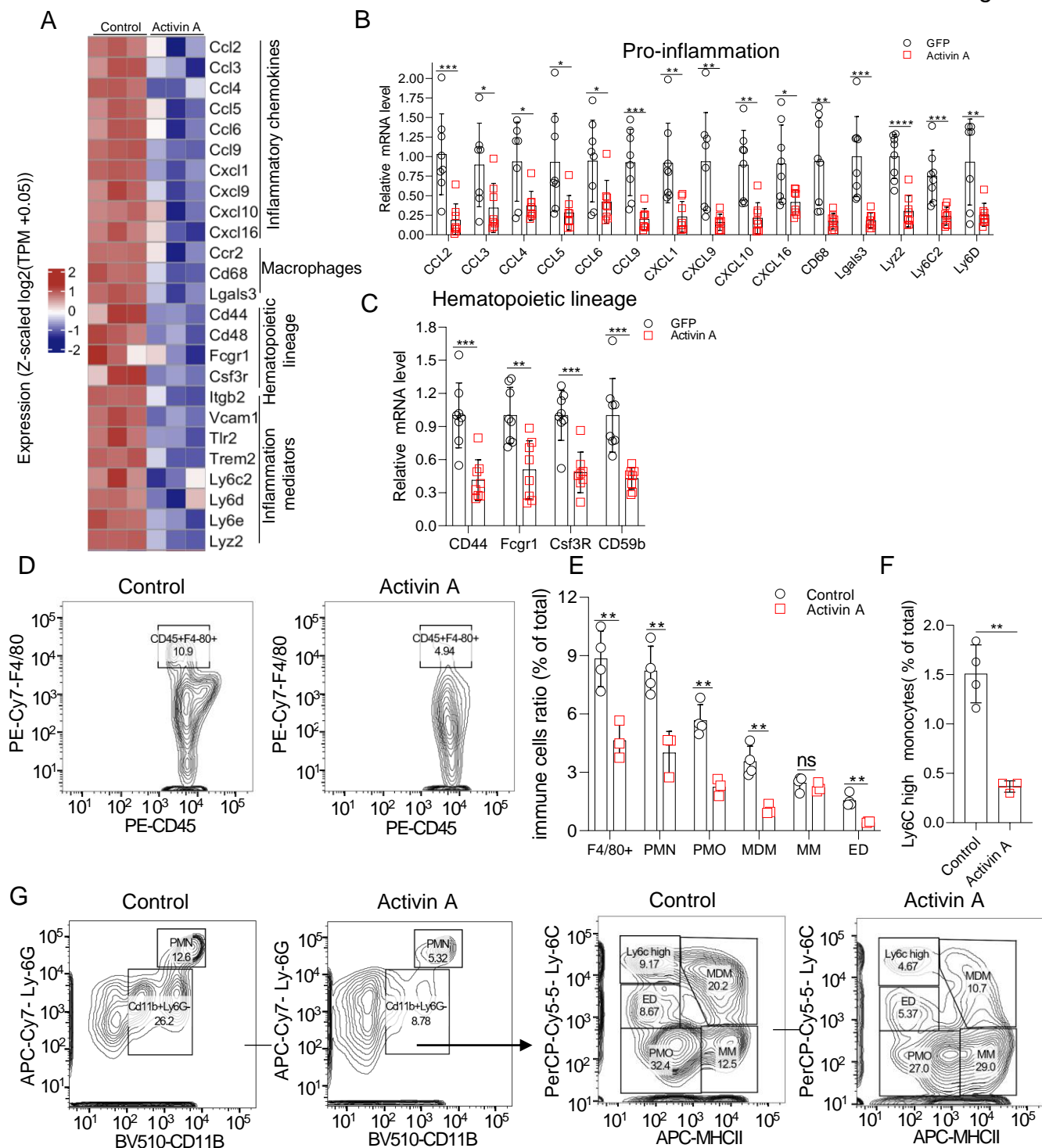
**H.** Quantification of relative Gpnmb, Srebp1, Srebp2, CD36 and Fabp5 protein level.

**I.** Images show the immunofluorescence staining of Gpnmb colocalization with CD45+ and F4/80+ cells, but not hepatocytes in atherosclerotic liver. CD45 (green), leukocytes marker, F4/80 (green), macrophages marker, Gpnmb (red), hepatocyte marker, HNF4 $\alpha$ , (purple, locates in nuclei), and nuclear stain DAPI (blue). Scale bar, 100 $\mu$ m.

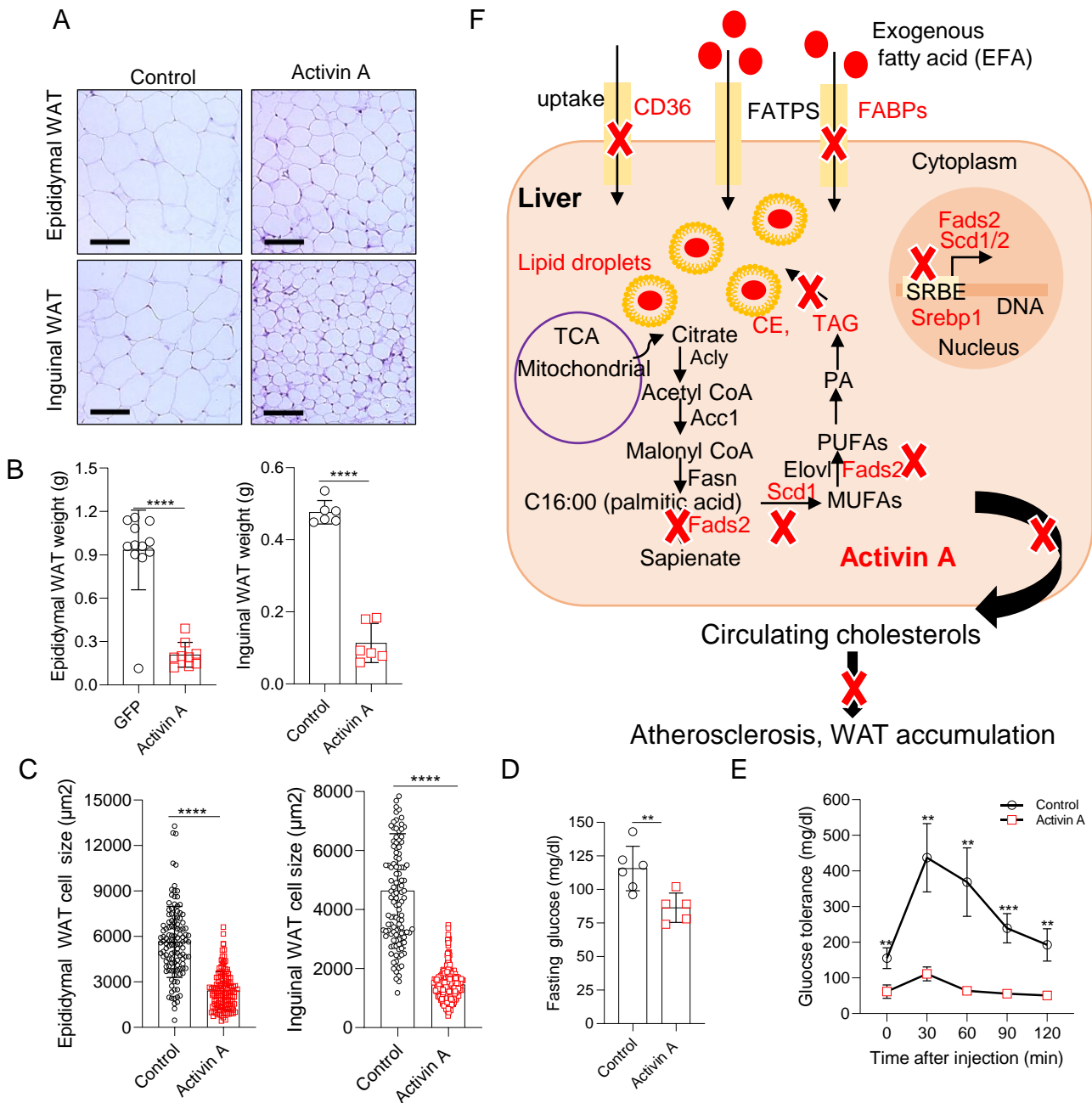
**J.** Quantification of Gpnmb+ cells in I. 4-5 random fields /section. N=5 mice.

**K.** Q-PCR shows decreased mRNA levels of lipid-associated-macrophages markers Trem2, Gpnmb and CD9 in Activin A-expressing liver compared with control. N=8 mice.

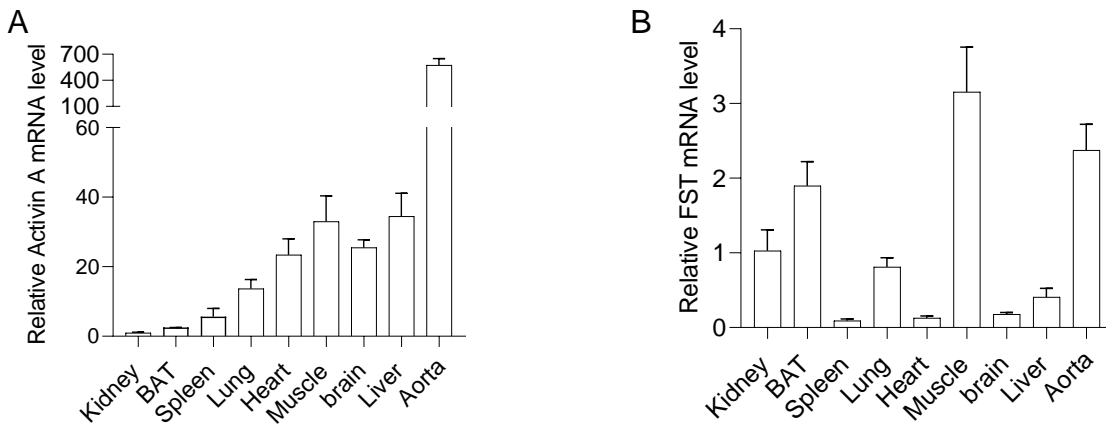
**L-M.** Assessment, gating strategy and quantification of lipid associated- macrophages (Trem2 high CD9+). Gpnmb antibodies did not work for flow. N=3-4 mice.



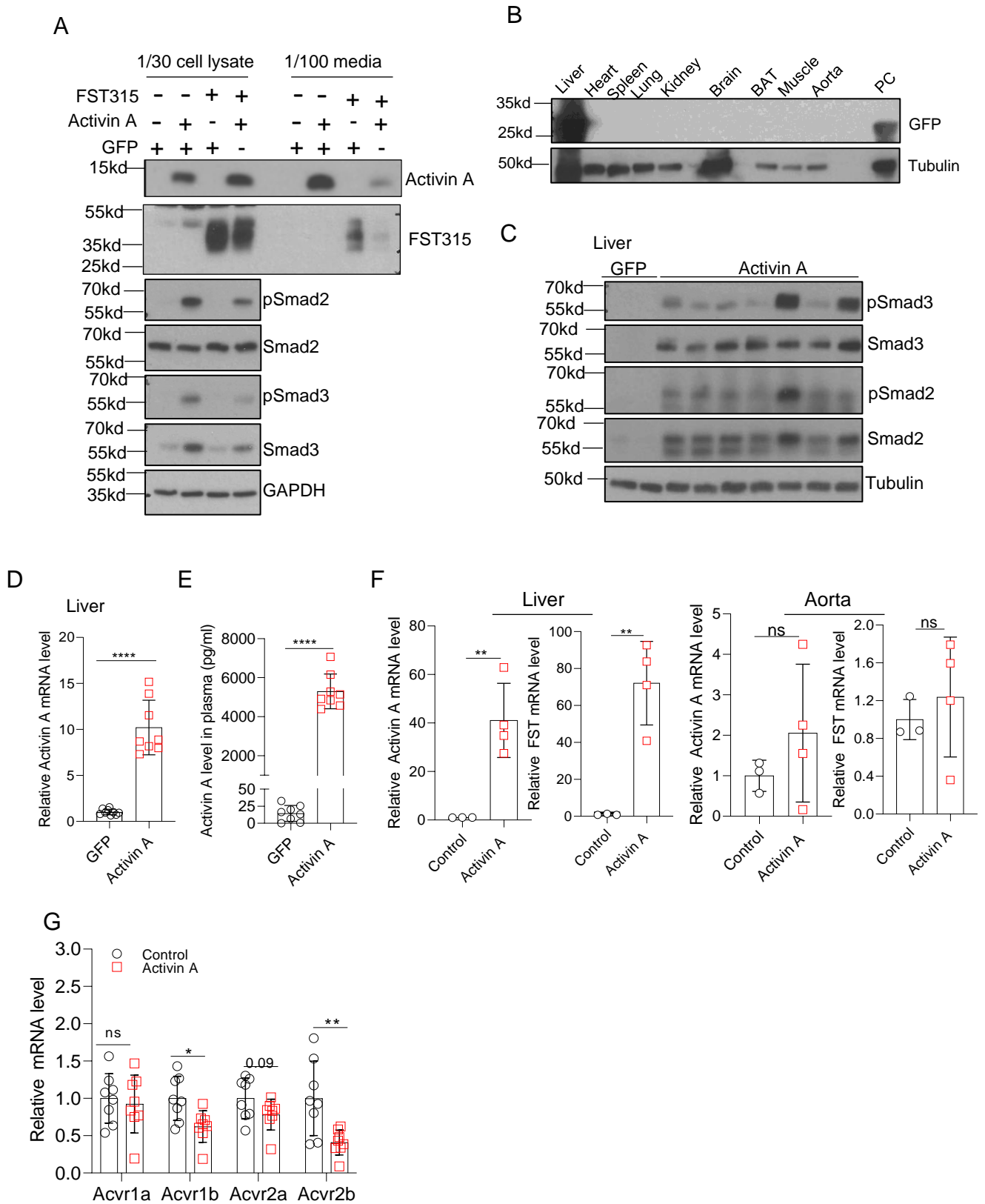
**Figure 5. Activin A decreases liver macrophages, Ly-6C<sup>high</sup> monocytes and polymorphonuclear cells (PMN) infiltration in Atherosclerotic mice.** **A.** Heatmap shows differentially regulated featured genes in leukocytes migration pathway. Gene list is from GO enrichment. Relative gene expression values (Z-scaled log<sub>2</sub>(TPM + 0.05)) for the 25 genes related to pro-inflammation. TPM (control) or TPM (Activin A) ≥ 5. p < 0.05, |log<sub>2</sub>Fc| ≥ 1, padj < 0.01. **B-C.** Q-PCR confirmation of RNA-seq data in A. **D.** Assessment of CD45+F4-80+ populations by flow cytometry. **E-F.** Quantification of immune cells from D and G. PMN (polymorphonuclear cells, CD45+CD11b+Ly-6G+, including neutrophils, basophils, and mast cells), PMO (patrolling monocytes, CD45+CD11b+ Ly-6G-Ly-6C- MHC-II-), MDM (monocytes-derived macrophages, CD45+CD11b+ Ly-6G-Ly-6C<sup>high</sup> MHC-II<sup>high</sup>), MM (mature macrophages, also known as Kupffer cells, CD45+CD11b+ Ly-6G-Ly-6C<sup>neg/low</sup> / MHC-II<sup>high</sup>), ED (eosinophils), Ly-6C<sup>high</sup> monocytes (CD45+CD11b+ Ly-6G-Ly-6C<sup>high</sup>/MHCII-). N=3-4 mice. Repeat for 3 times. **G.** Assessment and gating strategy of immune cells in atherosclerotic liver by flow cytometry in E and F.



**Figure 6. Activin A inhibits fat accumulation and improves glucose tolerance.** **A.** Representative Hematoxylin and Eosin staining of epididymal White Fat Tissue (WAT) and inguinal WAT in Activin A treated mice compared with Control. N=7 for Inguinal WAT and N=11-12 in epididymal WAT. Scale bar: 50 $\mu\text{m}$ . **B.** Quantification of the WAT weight in Activin A delivered mice compared with Control. Unilateral fat was calculated. N=6-12 mice. **C.** Quantification of inguinal WAT and epididymal WAT adipocyte areas. N=7 mice. **D.** Fasting glucose level was measured by a glucose meter and strips. Mice were fasted for 5 hours before the measurement. N=5-6 mice. **E.** Glucose tolerance was measured by a glucometer. Overnight-fasted mice were injected intraperitoneally with glucose (2 g per kg body weight). Blood glucose levels were measured at the basal level and at 15, 30, 60, 90 and 120 min after glucose administration using a blood glucometer. N=3-4 mice. **F.** A schematic model of the role of Activin A in regulating the metabolic processing of fatty acid in the liver, and effects on circulating cholesterol levels and atherosclerosis. Activin A not only blocks genes involved in fatty acid uptake including CD36 and FABPs, but also attenuates expression of genes involved in fatty acid *de novo* lipogenic pathways including Srebp1-Scd1/Fads2. Pathways expected to be downregulated by Activin A are indicated with a red X. Scd1/Scd2 and Fads2 expression are regulated by Srebp1 at the transcriptional level. ACLY, ATP-citrate lyase; ACC, acetyl-CoA carboxylase; FASN, fatty acid synthase; ELOVLs, elongation of very long-chain fatty acid protein; PA, phosphatidic acid; TAG, triacylglycerol; CE, cholesterol ester.



**Figure S1, related to Figure 1. A-B.** mRNA levels of Activin A and FST measured by QPCR in different tissues in mice.



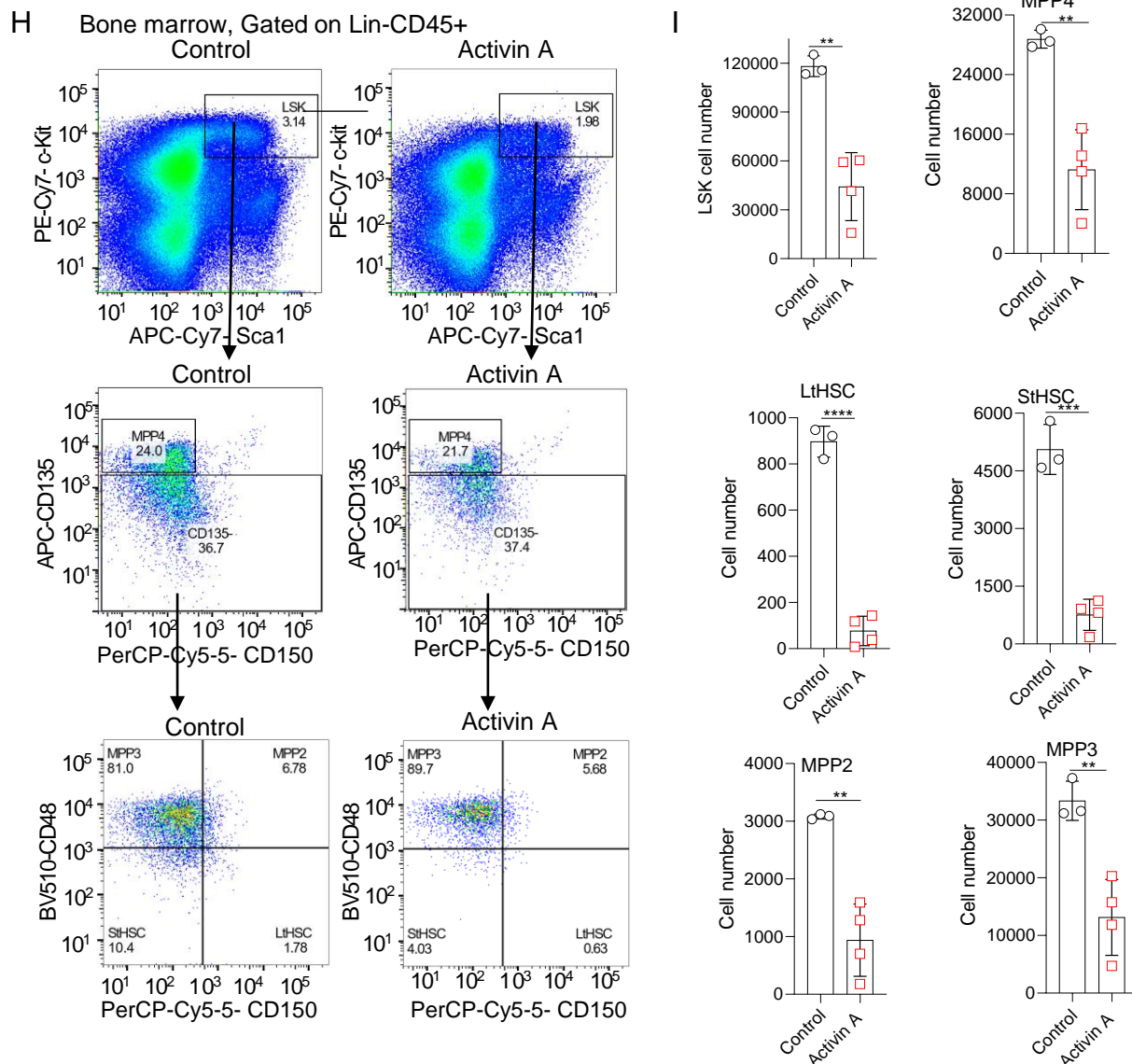


**Figure S2, related to Figure 2. A.** Western blotting showing that AAV8-TBG-Activin A is expressed in HepG2 cells, activates Smad2/Smad3 phosphorylation, and circulates in the media, while AAV8-TBG-FST315 blocks the activity of Activin A. The indicated plasmids were transfected into HepG2 cells and cultured for 48 h. **B.** Western blotting shows AAV8-TBG-GFP was highly expressed in liver but no other tissue after tail vein injection. 6-week-old male C57/BL6 mice were I.V. injected with  $5 \times 10^{10}$  AAV8-TBG-GFP, and then sacrificed after 4 weeks. Protein levels were quantified and normalized by BCA kit (pierce), and target proteins were detected by western blotting using anti-GFP antibody. HepG2 cell lysates with GFP expression were used as the positive control (PC). 18.74  $\mu\text{g}$  protein /sample. **C-D.** Western blotting and Q-PCR show AAV8-TBG-Activin A was expressed and activated the Activin pathway. 6-week-old male C57/BL6 mice were I.V. injected with  $5 \times 10^{10}$  genome copies AAV8-TBG-GFP, and then sacrificed after 4 weeks. Protein level was quantified by BCA kit (pierce) and target proteins detected by western blotting. **E.** ELISA shows liver expressed Activin A circulates in plasma. Mice from H were used. Plasma FST levels are close to baseline (0) and not shown here. **F.** Q-PCR shows AAV8-TBG-Activin A is expressed and induces expression of its direct target gene FST in the liver but not aorta in atherosclerotic LDLR<sup>-/-</sup> mice. Control, n=3 and Activin A, n=4. **G.** Q-PCR shows the mRNA levels of Activin pathway receptors in control and Activin A-expressing atherosclerotic liver. N=8 mice. Acvr1a, Acvr1b, Acvr1c, Acvr2a and Acvr2b primers were used for Q-PCR, and Acvr1c was undetectable. **H.** Assessment and gating strategy of hematopoietic stem cells (HSC) populations by flow cytometry. LSK: Lin<sup>2</sup>-CD45<sup>+</sup>Sca1<sup>+</sup>c-Kit<sup>+</sup>. Long-term HSC (LtHSC), short-term HSC (StHSC) and multipotent progenitors (MPP2, MPP3 and MPP4). StHSC (CD135-/CD150-/CD48- LSK), LtHSC (CD135-/CD150+/CD48- LSK) MPP2 (CD135-/CD150+/CD48+ LSK), MPP3 (CD135- /CD150-/CD48+ LSK), and MPP4(CD135+/CD150-/CD48+/- LSK). **I.** Quantification of the number of LSK, LtHSC, StHSC and multipotent progenitors in control and Activin A-expressing atherosclerotic mice. N=3-4 mice. Similar results were obtained from 3 independent experiments.

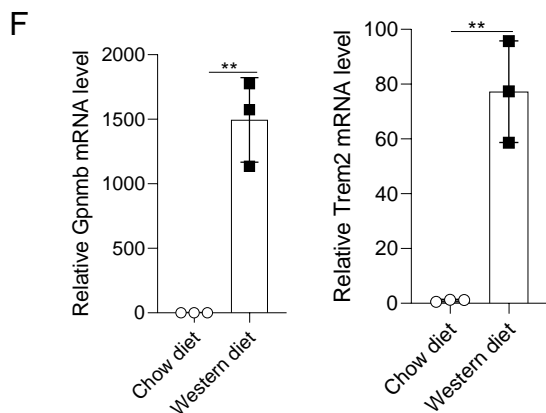
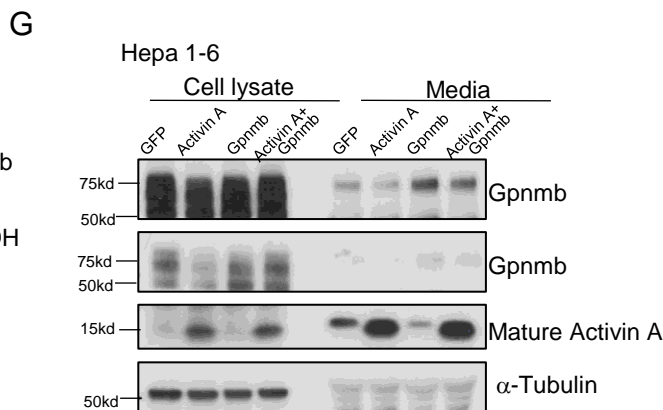
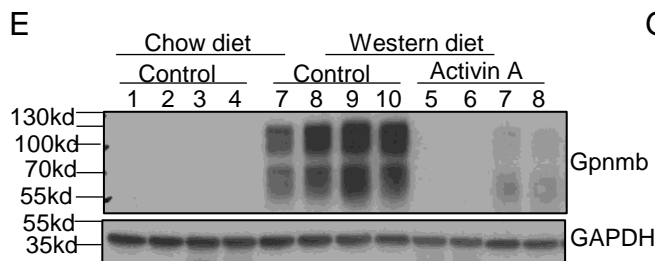
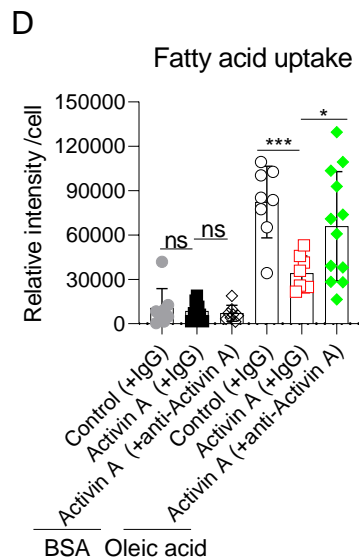
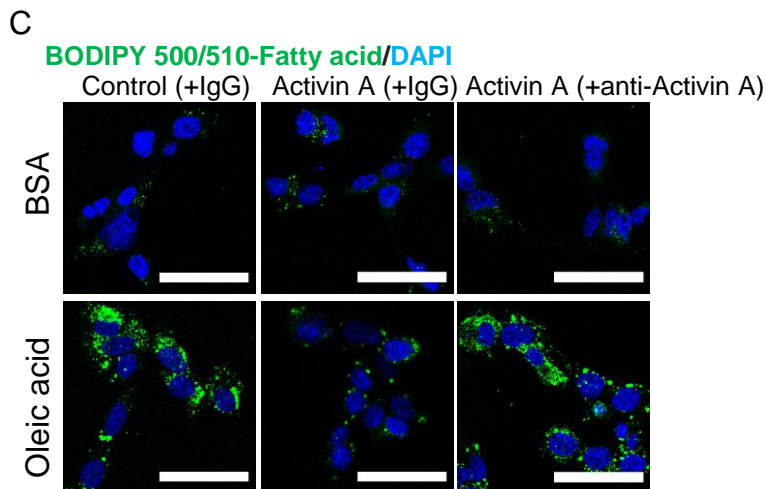
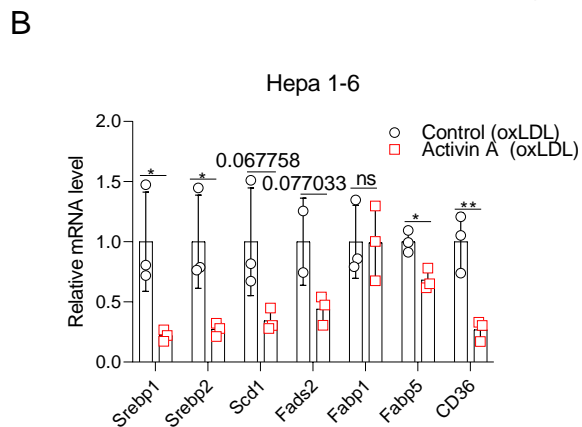
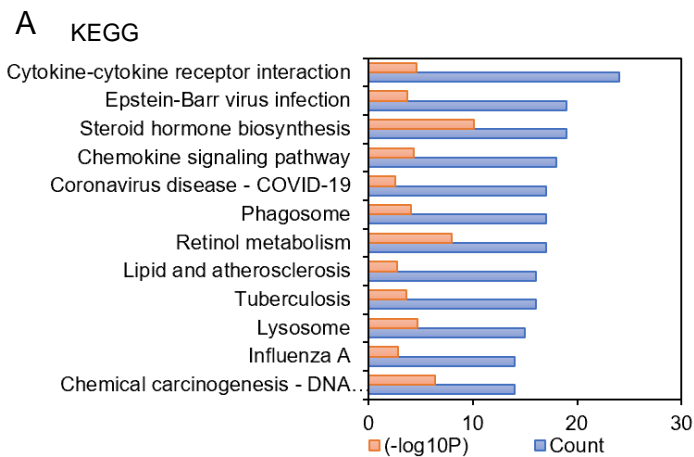


**Figure S3, related to Figure 4. A.** KEGG enrichment of top 12 significantly changed pathways in RNA-seq analysis of Activin A-expressing liver compared with control. TPM (control) or TPM (Activin A)  $\geq 5$ ,  $p < 0.05$ ,  $|\log_2 F_c| \geq 1$ . **B.** Q-PCR shows the mRNA levels of genes for hepatic *de novo* lipogenesis and exogenous fatty acid uptake decrease in Hepa 1-6 cells treated with Activin A-expressing conditioned media and 10  $\mu\text{g/ml}$  oxLDL compared with control. Hepa 1-6 cells were transfected with TBG-GFP or TBG-Activin A plasmid, and 24h later were changed into 0.5%BSA (fatty acid free)/RPMI at 37°C for 24h. The conditioned media were collected and filtered through a 0.22  $\mu\text{m}$  filter, diluted twice with fresh 0.5%BSA/RPMI1640, and then added into fresh Hepa 1-6 cells together with 10  $\mu\text{g/ml}$  oxLDL for 24 hours. **C-D.** Confocal images and quantification of fatty acid uptake. Hepa 1-6 cells were transfected with TBG-GFP or TBG-Activin A plasmid, and 24h later were changed into 0.5%BSA (fatty acid free)/RPMI at 37°C for 24h. The conditioned media were collected and filtered with a 0.22  $\mu\text{m}$  filter, diluted twice with fresh 0.5%BSA/RPMI1640, and then added into fresh Hepa 1-6 cells, with or without 30  $\mu\text{M}$  Oleic acid (OA), with 1  $\mu\text{g/ml}$  Mouse IgG1 Isotype Control or neutralizing anti-Activin A antibody for 24 hours. Then cells were washed with PBS, stained with 2  $\mu\text{M}$  BODIPY 500/510-fatty acid, fixed with 4%PFA, and stained with DAPI. Scale bar, 50  $\mu\text{m}$ . **E.** Western blotting shows Gpnmb is expressed in western diet-fed LDLR<sup>-/-</sup> control mice compared with chow but decreases in Activin A-expressing western diet-fed LDLR<sup>-/-</sup> mice. **F.** Q-PCR shows Gpnmb and Trem2 mRNA increase in western diet-fed LDLR<sup>-/-</sup> mice compared with chow diet. **G.** Western blotting shows Activin A decreases Gpnmb protein levels in cell lysate and media.  $\alpha$ -Tubulin as the loading control.